Lactation and gestation controls on calcium isotopic compositions in a mammalian model

Auguste Hassler, Jeremy E Martin, Stéphane Ferchaud, Doryan Grivault, Samuel Le Goff, Emmanuelle Albalat, Jean-Alexis Hernandez, Théo Tacail, Vincent Balter

This is an early version. Substantial changes in the content are available from the definitive version: https://doi.org/10.1093/mtomcs/mfab019

Lactation and gestation controls on calcium isotopic compositions in a mammalian model

Authors

Auguste Hassler[a]*, Jeremy E. Martin[a], Stéphane Ferchaud[b], Doryan Grivault[b], Samuel Le Goff[a], Emmanuelle Albalat[a], Jean-Alexis Hernandez[c], Théo Tacail[d], Vincent Balter[a]

[a] Univ Lyon, ENSL, Univ Lyon 1, CNRS, LGL-TPE, F-69007 Lyon, France

[b] GENESI, INRA, Rouillé, France

[c] Center for Earth Evolution and Dynamics, University of Oslo, N-0315 Oslo, Norway

[d] Bristol Isotope Group, School of Earth Sciences, University of Bristol, Bristol, BS8 1RJ, UK

* Corresponding author: auguste.hassler@ens-lyon.fr

Abstract

Lactation and gestation are among the physiological events that trigger the most intense changes in body calcium (Ca) fluxes. Along with the composition of the animal diet, these events are suspected to impact the Ca isotopic composition of Ca body reservoirs but their dynamics are poorly understood. In this study, we monitored a group of domestic sows across a full reproduction cycle. We collected tissues and fluids (blood, urine, milk, colostrum, umbilical blood, adult and piglet bones) at different steps of gestation and lactation, and analyzed their Ca isotopic compositions (i.e. $\delta^{44/42}Ca$) by mean of MC-ICP-MS. Among other results, we report the first observations of Ca isotopic fractionation between

maternal and umbilical blood ($\Delta^{44/42}Ca_{\text{umbilical blood- sow blood}}$ = -0.18 ± 0.11 ‰, n = 3). Our data also highlight that gestation and lactation periods are characterized by small diet-bone Ca isotopic offsets ($\Delta^{44/42}Ca_{\text{bone-diet}}$ = -0.28 ± 0.11 ‰, n = 3), with ^{44}Ca-enriched blood compositions during nursing ($\Delta^{44/42}Ca_{\text{nursing blood-gestation blood}} = +0.42^{+0.11}_{-0.12}$ ‰, n = 3). Under the light of an up-to-date mammalian box model, we explored different scenarios of gestation and lactation Ca fluxes experienced by a sow-like animal. These simulations suggest that gestation changes on body $\delta^{44/42}$Ca values result from the intensification of Ca absorption by the animal, whereas the production of ^{44}Ca-depleted milk is the main driver for the ^{44}Ca enrichment in blood during lactation. In addition, our results also support that bone mineralization could be associated with a more restricted Ca isotopic fractionation than previously envisioned. Together, these results refine the framework of Ca isotope applications, notably regarding the monitoring of human bone balance and the study of species and ecosystems from the present and the past.

1. Introduction

There is evidence that the Ca isotopic composition of mammal bone and teeth is controlled by diet, but other physiological parameters might also be at play and the cycling of Ca and its isotopic fractionation in the body is far from being fully understood [1–17]. Among dietary inputs, milk is highly depleted in heavy Ca isotopes relative to adult diet ($\Delta^{44/42}Ca_{\text{milk-diet}}$ = -0.6 ‰)[13], the consumption of milk affects the Ca isotopic composition of juvenile teeth, which can be used to document weaning ages and nursing practices [15,18,19]. Nevertheless, the production of milk (lactation) and possibly gestation seem to affect bone and blood Ca isotopic composition of breeding females [9,14], notably by generating male versus female differences in bone Ca isotopic composition ($\Delta^{44/42}Ca_{\text{females-males}}$ = +0.14 ± 0.08 ‰)[14]. Until now,

this phenomenon has only been described for sheep whereas there is no evidence of such sexual difference in human populations [8,14]. It may not be surprising that different mammal species display different sexually driven isotopic differences due to their physiological and behavioral differences. However, this observation calls for further investigations on other mammal species and, more essentially, on physiological factors at play to generate these sexually driven isotopic differences. Improving our knowledge about the mammalian Ca isotope cycle is motivated both by the development of biomedical innovations based on Ca isotope measurements [6,20–24] and potential applications in paleoanthropology and paleontology [1,2,10,13–15,18,19,25,26]. For example, new methods for bone balance and osteoporosis monitoring depend upon an accurate description of the Ca isotope cycle [6,20–24]. Besides, sexually driven Ca isotopic differences could help in detecting sex or past lactation events from teeth or bones, if their causing factors could be further constrained and quantified [14]. This would be a great opportunity for paleontologists as these are challenging to detect by other means. Finally, clearly identifying the range of action of these factors seems to be a necessary step to accurately reconstruct dietary preferences from Ca isotopic compositions within mammalian faunas [1,7,10–12,14].

The hypothesis that sexual differences of bone Ca isotopic compositions originate from gestation, lactation or both, arise from experiments and modeling, which suggest important Ca isotopic fractionation during milk production (notably inferred from the $\Delta^{44/42}Ca_{milk\text{-}diet}$ of -0.6 ‰)[13] and bone mineralization[2,5,9,13,14,17] (notably inferred from the $\Delta^{44/42}Ca_{bone\text{-}diet}$ of -0.57 ± 0.10 ‰, n = 21; see review from [2]). In this scenario, milk is enriched in light Ca isotopes relative to blood, and bone growth associated with gestation preferentially favors light Ca isotopes during the mineralization process [14]. However, later studies have highlighted that fractionation of Ca isotopes also occurs during urine formation through the reabsorption of

Ca from primary urine by kidneys [17,21–23,27,28], as evidenced by differences between blood and urine $\delta^{44/42}Ca$ values ($\Delta^{44/42}Ca_{urine\text{-}blood}$ = +1.15 ± 0.06 ‰, n = 29)[3,17,21,23]. In parallel, small differences between blood and bone Ca isotopic compositions in humans, sheep and rats [3,27] (i.e. ≤ 0.3 ‰) and new modeling integrating Ca urinary fractionation in normal conditions (i.e. without gestation or lactation related Ca fluxes; see [3]) also suggest a reevaluation of Ca fractionation amplitude at bone mineralization [2,3]. It is thus necessary to integrate these findings in updated models in order to unravel the underlying causes behind the observed sexual differences in Ca isotopic composition, as well as to provide guidance for future investigations of such gestation and lactation signals. It is also essential to widen the spectrum of mammals for which such difference is documented experimentally in order to test modeling predictions. The aim of this study is to address both of these aspects, by documenting the effects of gestation and lactation on Ca isotopic composition in the domestic pig, *Sus scrofa domesticus*, and by comparing these data with stable isotope box-models that consider urinary isotopic fractionation along with other fractionation processes described so far for Ca.

To achieve these objectives, we designed a breeding and feeding experiment consisting of a close monitoring of three adult sows during a full reproduction cycle. Over the 6 months of the experiment, samples including blood, urine, milk, colostrum, umbilical blood and bone have been collected while maintaining a diet with a stable Ca isotopic composition. This controlled environment allows us to identify the physiological drivers of Ca isotopic compositions in body reservoirs at each step of the reproduction cycle. Our sampling procedure allows us to compare the Ca isotopic composition of different body reservoirs at rather high temporal resolution, and to monitor the evolution of their respective Ca isotopic composition before, during, and after gestation and lactation periods. Attention was also

given to the juveniles of these three individuals, notably to their weight, in order to estimate Ca transfers during gestation and milk production. Shortly after parturition, two piglets from other females living in the same conditions unfortunately died. We sampled the bones of these two individuals and measured their Ca isotopic composition in order to assess the isotopic fractionation occurring between mother and offspring bones during gestation. Using these results and literature data about pig Ca cycle during reproduction, we performed different box model simulations to compare with our experimental data. Finally, we use these comparisons to identify the main drivers of Ca isotopic fractionation in the body, and compare our findings with previous studies from pig, deer, mice, rat, sheep and human [3,8,9,13,14,17].

2. Material and method

2.1. Animal monitoring and sampling

The use of animals for scientific purpose has been authorized in accordance with the French rural and sea fishing code, notably following the articles R.214-87 and R.214-126. The ethical approval was given to the project (referenced as APAFIS#13631-2018021417118920 v3) by the ethics committee of animal experimentations N°084. Sampling procedures have been designed to minimize animal stress and to be the least invasive possible. Moreover, this study has been grafted to an already going agronomic study, therefore preventing supplementary animal use.

The three monitored sows (C1, C2 and C3) were crossbred Landrace Français and Duroc breeds, raised within the unit of Genetic, experimentation and innovative systems (GenESI) of the French National Institute for Agriculture, Alimentation and Environment Research (INRAE), in the facility of la gouvanière (Rouillé 86480, France, DOI:

10.15454/1.5572415481185847E12). Two were at their second breeding cycle (C1 and C3 individuals), another was at its third breeding cycle (C2). The experiment started 12 to 14 days after the weaning of a previous litter, a breeding cycle conducted within the same environment with a similar diet made up of a mix of barley, corn, wheat, sunflower, rapeseed, beets, sugar cane, calcium carbonate as well as other minor ingredients constituting about 1% of the mix (e.g. sodium chloride and sodium bicarbonate). The return to estrus during this 14 days period has been artificially delayed by administrating Régumate® to sows for about the first 10 days after weaning. One other individual (C8) living in the same conditions died from an unidentified cause between the experiment and the previous breeding cycle. We collected one of its phalanxes to perform comparative bone analyses. The blood, urine, colostrum, milk of sows and umbilical blood from their piglets were collected at 5 key moments of their reproduction: 3 days before the insemination, during the last month of gestation, shortly after parturition, during nursing and 14 days after weaning (figure 1). At each step, bio-fluids were collected with the intention to minimize the time lapse between each collection, in order to maximize the comparability between samples from Ca reservoirs with small Ca residence time. To the same end, all sampling sessions were carried in the morning, before the first meal and after at least 8 hours of fasting. This procedure allows to minimize short term impacts of food intakes on Ca isotopic compositions of body reservoirs. We maintained the same food supply and performed food samplings during the duration of the experiment to monitor the isotopic variability of sow Ca intakes.

Sampling sessions were conducted as follows. On sampling days, light was switched on manually at the arrival of the collecting team, under the supervision of S. Ferchaud and D. Grivault. Urines were preferably collected with the first urination of the day, as an attempt

to limit the impact of urine isotopic variability over day-time and because 24h urine collections were not achievable. Urines were collected in Falcon® tubes (50 mL, REF 352070) without the first milliliters of the urination, then transferred in 2 ml polypropylene (PP) tubes and stored in a freezer. This step requires a close monitoring of sows to achieve the collection, a success upon which subsequent samplings were initiated or not. For blood collection, adult individuals were immobilized then blood was collected from the jugular vein using lithium heparin tubes without gel (BD Vacutainer®, REF 367526). Blood samples were centrifuged, then the plasma was collected and transferred in PP tubes prior to be store-frozen. Because almost all the Ca from the blood is contained within the plasma [3,29–31], plasma and total blood Ca compositions are considered to be identical in this article. At parturition, umbilical blood was collected from umbilical cords in heparin tubes without gel (BD Vacutainer®, REF 367526). The umbilical plasma has been collected after centrifugation and stored in the same conditions than regular plasma. At parturition and 14 days after parturition, respectively 4 ml of colostrum and 2ml of milk were collected from each individual. These collections were achieved in PP tubes by operating a massage of the udder. No hormonal injection was carried on in that purpose. Fourteen days after the weaning of their offspring and after a last round of sampling, studied animals were slaughtered to join the traditional circuit of pork meat distribution. Their skulls were collected, boiled in water and manually cleaned to allow bone sampling from their mandible using a handled drill (8200 Dremel with tungsten steel solid carbide bit).

2.2. Weight and milk production estimates

We estimated the weight of the three studied sows based on the average weight recorded for their congeners in the INRAE GenESI facility. At weaning of their second lactation, sows from the same breed weigh 199.3 ± 17.1 kg (n = 117, ± standard error) on average, while

weighing an average of 213 ± 20 kg (n = 100, ± standard error) after their third lactation. This is similar to what is documented in Dourmad et al. (1997)[32] and Giesemann et al. (1998)[33], who support that Ca reservoir sizes and Ca fluxes reported in these studies are of the same order of magnitude than for the individuals of our experiment. At birth, piglets were weighed to estimate the amount of Ca they received from their mother during gestation. This estimation is based on the assumption that dry bone represents about 4.88% of their total body mass (mean calculated from two newborns of the same breed) and that Ca accounts for about 26.58% of bone mass (extrapolated from cow bone meal reference material NIST SRM1486). After birth, litters were rearranged between sows from within and outside the experiment, in order to equilibrate the number of piglets per sow and guarantee healthy growth conditions. The piglet mass gain at weaning is thus calculated while including all piglets (native and adopted) nursed per each sow, by subtracting their weight at weaning by their weight at birth. This piglet daily weight gain (referred as GMQ to match the notation of Etienne et al., 2000[34]) is used to calculate the piglet daily intake of milk dry fraction (referred as MS to match the notation of Etienne et al., 2000[34]) using the following formula: MS = 0,72 (± 0,07) x GMQ – 7, where MS and GMQ are expressed in gram/piglet/day [34]. Considering an average sow milk dry mass fraction of 18% [34,35] allows to estimate sow average milk daily production. Five piglets died between birth and weaning with a noticeable weak body condition. Their puny state at death supports that they consumed limited amounts of milk and that their body mass can be neglected in the calculation of milk production.

2.3. Sample preparation and chromatography

Complementary details regarding equipment and cleaning procedures used in this study can be found in appendix A.1, the following section focus on the operations performed on

188 samples, blanks and reference materials. Prior to chromatography and concentration
189 analyses, blood, colostrum, milk and food samples have been freeze-dried, homogenized in
190 an agate mortar, weighed and placed in Perfluoroalkoxy (PFA) beakers (Savillex®). Urine
191 samples have been unfrozen and homogenized, then 500 µL of each were collected in PFA
192 beakers. Bone powders collected from mandibles were weighed and placed in PFA beakers
193 prior to digestion. Further manipulations were carried exclusively in a clean lab, under a
194 laminar flux hood (absolute filter H14) to avoid environmental contamination. After being
195 placed in PFA beakers, samples were mixed with 10 ml of distilled nitric acid (15 M, Fisher
196 Scientific®, Primar plus® – Trace analyses grade, in-house distilled) and 1 ml of 30 % suprapur
197 hydrogen peroxide (H_2O_2, Fisher Chemical®, Hampton, NH, USA) to start digestion. Samples
198 were left at ambient temperature for 1h, then placed on a hotplate at 160 °C for two days
199 and evaporated to dryness. All along this procedure, we performed periodic beaker
200 degassing to avoid critical overpressure. This procedure was repeated at least three times,
201 until complete mineralization of samples. The complete digestion of the organic matter was
202 assessed by monitoring H_2O_2 effervescence. Digested and evaporated samples were
203 dissolved in 0.5 M distilled HNO_3 (Fisher Scientific®, Primar plus® – Trace analyses grade, in-
204 house distilled), a fraction of which was kept for concentration analyses. The rest has been
205 evaporated to dryness, dissolved in 6 M distilled hydrochloric acid (Fisher Scientific®,
206 laboratory reagent grade, in-house distilled), and evaporated again prior chromatography.

207 The chromatography procedure used for Ca chemical purification is derived from Tacail et al.
208 (2014)[27] and Le Goff et al. (2021)[36]. It consists in a triple column chromatography, starting
209 with an elution on AG1 X8 resin to discard elements such as Zn and Fe, followed by an AG
210 50WX-12 resin to isolate Ca and strontium (Sr) from the matrix, and by an elution on
211 Eichrom Sr-specific resin to isolate Ca from Sr. This procedure is detailed in Table B.1. Blanks

have been monitored all along digestion and chromatography processes (i.e. total and chromatography blanks) to control for Ca contamination levels. The use of heparin tubes for blood collections (BD Vacutainer®, REF 367526) LH, is associates with additional Ca contaminations. To estimate this contamination, we filled a heparin tube of MilliQ (Millipore®, initial resistivity = 18 MΩ.cm at 25 °C) during one hour at ambient temperature, and analyzed its Ca concentration by mean of ICP-MS.

2.4. Analytical procedures

Elemental concentrations have been measured on an inductively coupled plasma atomic emission spectrometer (ICP-AES, model ICAP 7400 Series, Thermo Scientific®), with the exception of the Ca content of heparin tubes which has been measured by mean of an inductively coupled plasma mass spectrometer (ICP-MS, model ICAP Q, Thermo Scientific®). The reliability of measurements has been controlled through a set of blanks and reference materials, as well as by replicating measures at least twice for each sample.

We measured Ca isotopic ratios ($^{44}Ca/^{42}Ca$ and $^{43}Ca/^{42}Ca$) using a multi-collector ICP-MS (MC-ICP-MS, Neptune Plus, Thermo Scientific®) following the method described in Tacail et al. (2014)[27]. Prior to Ca isotopic analyses, Ca purified samples were dissolved in distilled 0.05 M HNO_3 in order to set the Ca concentration at 1.25 $mg.L^{-1}$. This concentration matches the concentration of our in-house bracketing standard, a Specpure Ca plasma standard solution (Alfa Aesar) named ICP Ca Lyon and described in previous studies [1,16,18,27]. Calcium isotopic composition reported in this article are all expressed as $\delta^{44/42}Ca$ values calculated based on this reference material and the following formula (unless explicitly mentioned):

$$\delta^{44/42}\mathrm{Ca} = \left(\left(^{44}\mathrm{Ca}/^{42}\mathrm{Ca}\right)_{\mathrm{sample}} / \left(^{44}\mathrm{Ca}/^{42}\mathrm{Ca}\right)_{\mathrm{ICP\ Ca\ Lyon}} - 1 \right) \qquad [1]$$

With $\delta^{44/42}Ca$ values given in ‰. For more comparability with studies from other laboratories, the $\delta^{44/42}Ca_{ICP\ Ca\ Lyon}$ values are also expressed as $\delta^{44/42}Ca_{SRM915a}$ in tables and figures. Based on 71 measures synthetized in the appendix of Martin et al. (2018)[10], we converted $\delta^{44/42}Ca_{ICP\ Ca\ Lyon}$ values to $\delta^{44/42}Ca_{SRM915a}$ values by adding +0.518 ‰ to $\delta^{44/42}Ca_{ICP\ Ca\ Lyon}$ values. This conversion is associated with a wider uncertainty interval corresponding to +0.025 ‰ of the uncertainty around $\delta^{44/42}Ca_{ICP\ Ca\ Lyon}$ values (error bars within figures reflect uncertainties around $\delta^{44/42}Ca_{ICP\ Ca\ Lyon}$ values only). We used the SRM1486, a cow bone meal reference material from NIST, as a secondary standard to assess the reproducibility of the ion-exchange chromatography procedure, as well as to monitor the accuracy of MC-ICP-MS measures. Blank Ca concentrations have also been measured using the Neptune Plus MC-ICP-MS. All samples and reference material measurements have been replicated at least three times (table B.6).

Differences between Ca isotopic compositions are expressed as $\Delta^{44/42}Ca$, following the formula:

$$\Delta^{44/42}Ca_{X-Y} = \delta^{44/42}Ca_{X} - \delta^{44/42}Ca_{Y} \qquad [2]$$

Where X and Y refer to different samples or Ca isotope reservoirs. For calculating $\Delta^{44/42}Ca$ values between sample types (e.g. blood, urine) at the scale of several individuals or sampling steps (e.g. the average $\Delta^{44/42}Ca$ value between blood and urine samples), the terms $\delta^{44/42}Ca_X$ and $\delta^{44/42}Ca_Y$ can simply be replaced by the mean $\delta^{44/42}Ca$ values of Ca reservoirs X and Y. Uncertainties expressed around $\Delta^{44/42}Ca$ values are the sum of the uncertainties of $\delta^{44/42}Ca_X$ and $\delta^{44/42}Ca_Y$. When a Ca flux connects two Ca reservoirs, the isotopic fractionation associated with this flux can be expressed as an isotopic fractionation factor α, calculated as follow:

$$\alpha_{X-Y} = \frac{\delta^{44/42}Ca_X + 1000}{\delta^{44/42}Ca_Y + 1000} [3]$$

Which can be approximated as:

$$1000 \times \ln(\alpha \| X-Y) \approx \delta^{44/42}Ca_X - \delta^{44/42}Ca_Y [4]$$

Where X and Y refer to different Ca isotope reservoirs connected by the Ca flux associated to the isotopic fractionation factor described by $\alpha_{X\text{-}Y}$.

2.5. Accuracy and precision of Ca isotopic compositions

For more clarity in the following sections, the n notation refers to a number of samples or specimens, whereas the n* notation specifically refers to number of replicates for a given measurement. Replicating Ca isotope measurements allows us to estimate the range of analytical precision of $\delta^{44/42}$Ca values. The correlation between $\delta^{43/42}$Ca and $\delta^{44/42}$Ca values for samples and reference materials follows the trend expected from an exponential fractionation law [37], with a slope value of 0.502 ± 0.007 (2 s.e.), an intercept of -0.003 ± 0.005 (2 s.e.), a R^2 = 0.997 and a p-value < 0.001 (figure C.1). This demonstrates that no mass independent fractionation or mass isobaric interference affect these measurements. Across the six days of analytical session with the MC-ICP-MS, the reference material SRM1486 exhibited a mean $\delta^{44/42}$Ca value of -1.01 ± 0.01 ‰ (2 s.e., n = 37), which is undistinguishable from previously published data for this reference material [10,18,38,39]. All these data support that the Ca isotopic compositions we measure are not biased by the ion-exchange protocol and MC-ICPMS setup, and that the measured Ca isotopic compositions are accurate.

For our bracketing standard (ICP Ca Lyon), blanks collected during the Sr purification step[27] represent about 100 ng of Ca, a negligible pollution at the scale of the 4 mg of Ca contained in the solution. For samples and SRM1486, chromatography blanks contain between 52 to

181 ng of Ca (~100 ng of Ca in average), while blanks monitoring environmental contaminations during the MC-ICP-MS session contain less than 10 ng of Ca. Heparin tubes can add about 273 ± 35 ng of Ca (2 s.e., n* = 2) to blood samples. For the majority of our samples these blank levels are negligible compared to the amount of Ca contained in samples, only 5 samples containing limited amounts of Ca could have been notably affected. Uncertainty estimations and corresponding error bars have been extended accordingly (table B.6). Equations behind uncertainties presented in this paper are described in details in appendix (text A.2).

2.6. Box model

In order to identify the mechanisms behind the distribution of Ca isotopic compositions in the body, we performed several simulations of a Ca box model using the Isopybox program. This Python-coded program derives from a code used in previously published work [40]. It iteratively calculates the evolution of isotopic compositions within interacting reservoirs of a given isotopic system [3]. In its current version, Isopybox allows to solve steady-state box model, study the relaxation time of a system in response to a discrete perturbation, and study the isotopic evolution of a system with unbalanced fluxes (providing that no box will be emptied during the duration of the run). The program and its resources are accessible on Github at the following address: https://github.com/ttacail/isopybox.git.

The conception of the model is described and discussed in further details in appendix (Text A.3; Tables B.2, B.3, B.4). In a few words, this model is a box model designed to simulate the Ca isotopic composition of a sow-like animal based on plausible Ca reservoir sizes, Ca fluxes and Ca isotopic fractionation factors. We modeled different scenarios of Ca fluxes and isotopic fractionation factors for the animal. First, we simulated a gestation without Ca

transfer to fetuses (Ca gain is transferred from extracellular fluids to the waste box with no isotopic fractionation). This simulation (referred as GestFF for Gestation Fetus Free) is purely conceptual but stay quite representative of the average conditions of a domestic sow, as the Ca transfer to fetuses intensifies only toward the last third of the gestation period, and that they generally have small nursing periods and recovery time between weaning and new insemination. The second simulation is similar to the first one but includes Ca transfer to fetuses (referred as GestR for Gestation Regular). This last aim to represent a sow toward the end of a gestation, when Ca transfer to fetuses are intense. The third and fourth simulations (LactA, LactB) represent a lactation scenario without bone loss, with relatively high (LactA) and low Ca dairy excretion (LactB). Finally, we tested the influence of Ca absorption (i.e. the amount of Ca transferred from the digestive tract to the blood) on body Ca isotopic compositions. This test is a series of simulations which use the basis of the GestFF scenario with different Ca absorption levels, respectively 75 %, 50 % and 25% of GestFF Ca fluxes from digestive tract to blood. In addition to these scenarios, we tested additional configurations of Ca fluxes and Ca isotopic fractionation factors in order to assess the sensitivity of the model to these parameters. Monitored parameters include: the coefficient of Ca isotopic fractionation at bone mineralization, the degree of bone loss, the ratio between Ca absorption and excretion (i.e. by digestive secretions) and the ratio between urinary and endogenous Ca losses. These last scenarios and associate results are further described in appendix (Text A.3; figures C.5, C.6, C.7).

3. Results

3.1. Zootechnical data

Zootechnical data for sows (e.g. litter size, weaning age, quantity of milk produced) from this study are reported in Table B.5. Estimations of sow body masses fall within the range of

body masses reported for other porcine specimens studied by Dourmad et al. (1997)[32] and Giesemann et al. (1998)[33]. The near four-month gestation of sows multiplied by the daily flux of extracellular fluids into the fetus (i.e. EF→Ft) documented by Giesemann et al. (1998)[33] produce estimations of total piglet Ca mass at birth which are lower but of the same order than the total piglet Ca mass estimated at birth for C1 and C3 offspring (Table B.5). In this experiment we estimate that sow produced an average of 10 kg of milk per day [34]. The fraction of Ca in milk samples was highly variable (3830 to 7632 ppm), which led to a wide range of possible Ca dairy output, from 8.16 to 16.25 g of Ca per day. Considering that Ca milk concentration is documented to be between 1700 and 2140 g/L after the second week of lactation [33,41], the upper estimation of 16.25 g/d of Ca dairy output seems more consistent and matches with Ca dairy outputs documented by Giesemann et al. (1998)[33]. Overall, the estimations of body masses, Ca reservoir size, placental and dairy Ca fluxes from this study are consistent with those reported in Giesemann et al. (1998)[33] and the other studies used to design the present model (Table B.2, B.3). This supports that these Ca flux data can be reasonably used within our model to compare with experimental measurements.

3.2. Experimental elemental and isotopic data

Calcium isotopic compositions collected during this study (205 measures for 50 sample and 1 reference material) are reported as both $\delta^{44/42}Ca_{ICP\ Ca\ Lyon}$ and $\delta^{44/42}Ca_{SRM915a}$ in figure 2 and table B.6. Food Ca isotopic composition remains consistently stable at -0.23 ± 0.06 ‰ (n = 3) during the duration of the experiment (figure 3a). Bones of adult females (C1, C2, C3) display $\delta^{44/42}Ca$ values distributed in a tight range between -0.49 ± 0.05 ‰ (n* = 4) and - 0.53 ± 0.05 ‰ (n* = 3), with a general $\Delta^{44/42}Ca_{bone\text{-}diet}$ offset of -0.28 ± 0.11 ‰ (n_{bone} = 3, n_{diet} = 3). Bones are undistinguishable from pre-insemination blood Ca isotopic compositions ($\Delta^{44/42}Ca_{bone\text{-}blood}$ ≈ -0.08 ± 0.11 ‰, n_{bone} = 3, n_{blood} = 3). The bone $\delta^{44/42}Ca$ value of the C8 individual (-0.51 ±

0.05 ‰, n* = 4) is indistinguishable from C1, C2 and C3 individuals. Milk Ca isotopic composition range between -0.70 ± 0.07 ‰ (n* = 3) and -0.96 ± 0.05 ‰ (n* = 3). The mean difference between the food of sows and their milk ($\Delta^{44/42}Ca_{milk\text{-}diet}$) is -0.58 ± 0.12 ‰ ($n_{milk}$ = 3, n_{diet} = 3), whereas the mean difference between their blood and milk during nursing ($\Delta^{44/42}Ca_{milk\text{-}blood}$) is -0.67 ± 0.12 ‰ ($n_{milk}$ = 3, n_{blood} = 3). Colostrum samples (n = 3) have a wider range of $\delta^{44/42}$Ca values than milk, from -0.72 ± 0.06 ‰ (n* = 3) to $-2.06^{+0.06}_{-0.05}$ ‰ (n* = 3), mainly because of one outlier sampled from the C3 individual. The two other colostrum samples (from C1 and C2) display $\delta^{44/42}$Ca values in the range of milk values (figure 2). Umbilical blood samples (n = 3) show intermediate $\delta^{44/42}$Ca values between mother blood and milk, ranging between -0.30 ± 0.05 ‰ (n* = 3) and -0.71 ± 0.05 ‰ (n* = 3). The mean $\Delta^{44/42}Ca_{umbilical\ blood\text{-}diet}$ offset is -0.29 ± 0.11 ‰ ($n_{umbilical\ blood}$ = 3, n_{diet} = 3). Close after parturition, the mean $\Delta^{44/42}Ca_{umbilical\ blood\text{-}\ sow\ blood}$ is -0.18 ± 0.11 ‰ ($n_{umbilical\ blood}$ = 3, $n_{sow\ blood}$ = 3) and -0.14 ± 0.11 ‰ for C1 ($n_{umbilical\ blood}$ = 1, $n_{sow\ blood}$ = 1), the individual for which collections of blood and umbilical blood were the closest in time. Thus, umbilical blood tends to be slightly depleted in heavy Ca isotopes compared to sow's food and blood (figure 2). Bone samples collected from the two early deceased piglets show a Ca isotopic composition undistinguishable from the adult sows, with a mean $\delta^{44/42}$Ca value of -0.50 ± 0.05 ‰ (n = 2). Urine Ca isotopic compositions range between $+1.27^{+0.05}_{-0.09}$ ‰ (n* = 3) and +0.55 ± 0.05 ‰ (n* = 3), with either a relative stability over time (C1 and C3 individuals) or a noticeable variability (C2 individual, see figure 3b).

We do not identify a common temporal pattern of urine Ca isotopic composition shared by the three individuals. Except for the C2 individual which shows higher urine $\delta^{44/42}$Ca values at parturition and post weaning steps, urine Ca isotopic composition seems relatively stable

over the experiment, although the data point of C2 is the only available for the post-weaning step (figure 3b). However, all individuals share a similar temporal pattern of blood Ca isotopic composition (figure 3c). Blood $\delta^{44/42}$Ca values range between -0.03 ± 0.06 ‰ (n* = 3) and -0.59 ± 0.06 ‰ (n* = 5). Depending on the individual, blood $\delta^{44/42}$Ca values are either stable or decrease between pre-insemination step (June) and the last month of gestation (early October). The amplitude of this change is between -0.01 ± 0.11 ‰ ($n_{pre\text{-}insemintation}$ = 1, $n_{syn\text{-}gestation}$ = 1) and -0.22 ± 0.11 ‰ ($n_{pre\text{-}insemintation}$ = 1, $n_{syn\text{-}gestation}$ = 1). However, the range of blood $\delta^{44/42}$Ca values between June and early October largely overlaps when all individuals are considered together. This period is followed by a rapid increase of $+0.42^{+0.11}_{-0.12}$ ‰ ($n_{syn\text{-}gestation}$ = 3, $n_{syn\text{-}nursing}$ = 3) in average between the last month of gestation (early October) and the middle of nursing (mid-November). The onset of this change in blood Ca isotopic composition is different between the individuals, with individual C3 exhibiting this offset 5 days after parturition whereas individual C2 still shows no sign of it 7 days after parturition (figure 3c). All the individuals consistently display this change 14 days after parturition (figure 3c). This phase is followed by a decrease of $-0.19^{+0.12}_{-0.13}$‰ ($n_{syn\text{-}nursing}$ = 1, $n_{post\text{-}weaning}$ = 1) to -0.34 ± 0.12 ‰ ($n_{syn\text{-}nursing}$ = 1, $n_{post\text{-}weaning}$ = 1) after weaning (late-November) depending on the individual. In the case of the C3 individual, blood $\delta^{44/42}$Ca values are back to initial values in December (respectively -0.58 ± 0.05 ‰ and -0.59 ± 0.07 ‰, n* = 3 for both).

Calcium concentrations in urine range from 2.8 to 715.9 mg/L. At the individual level, urines collected before insemination are systematically the most Ca concentrated. Ca concentration then decreases during the gestation, increases in the middle of the lactation period and goes back to post-birth levels after weaning (figure C.2). We found a weak linear and logarithmic correlation between urine Ca concentration and isotopic composition with a R^2 of 0.37 and

0.35, respectively (figure C.3). We found no significant temporal pattern of blood Ca concentration (figure C.2), or correlation between blood Ca concentration and isotopic composition (figure C.3). All non-blood samples isotopic compositions are shown compared to individual's blood compositions ($\Delta^{44/42}Ca_{X\text{-}blood}$) in figure C.4. The mean $\Delta^{44/42}Ca_{urine\text{-}blood}$ offset is $+1.21^{+0.11}_{-0.13}$ ‰ (n_{urine} = 12, n_{blood} = 12), which is undistinguishable from the offset of +1.15 ‰ used in our model. This offset, however, changes over time, notably during the lactation period when a cluster of low $\Delta^{44/42}Ca_{urine\text{-}blood}$ can be distinguished (figure 4).

3.3. Box model predictions

The structure of the box model of this study is detailed in figure 5. The evolutions of Ca isotopic compositions within some of these Ca reservoirs (i.e. extracellular fluids, urine, faeces, bone, milk and bulk fetus tissues) are presented in figure 6 and are the result of GestFF, GestR, LactA and LactB simulations. The initial conditions of these simulations are summarized in tables B.2, B.3, B.4, briefly described in section 2.6. and further detailed in the appendix section (Text A.3).

In figure 6, three phases can be distinguished for all the four simulations. From day 2 to day 100, extracellular fluids, urines, milk and fetal tissues reach a transient/temporary equilibrium, which depends strictly on Ca fluxes and associated Ca isotopic fractionation but not on initial Ca isotopic compositions. This result is expected considering the small Ca residence time of these reservoirs or their small initial size (e.g. fetal tissues). Our model thus predicts a rapid reaction of these reservoirs and a relative stability of the Ca isotopic composition within this time range. After 100-days and up to 10^4 days, we observe a change in bone Ca isotopic composition which also results in a slight increase of $\delta^{44/42}Ca$ values of extracellular fluids, urines, milk and fetal tissues. After 10^4 days, the sow system (not

420 including the fetus box) is relaxed to its steady state. We compared the four modelled
421 predictions with our experimental data, at different timings (100-days and steady state)
422 while considering different Ca isotopic fractionation factors ($\alpha_{B\text{-}EF}$) at bone mineralization
423 (figure 7, see table B.4 and reference therein). At steady state, only bone Ca isotopic
424 composition is affected by $\alpha_{B\text{-}EF.}$ This parameter has little impact on intermediate composition
425 states at 100-day for lactation but a more pronounced impact for gestation simulations
426 (figure C.5).

427 GestFF predictions for urine and extracellular fluids fits remarkably well within the range of
428 urine and blood data obtained from pre-insemination samplings (figure 7). Ca isotopic
429 compositions recorded in bones collected from sows after the weaning of the offspring fit
430 with compositions predicted from GestFF simulation, but only for Ca isotopic fractionation
431 factor $\alpha_{B\text{-}EF}$ between 1 and 0.9999 (i.e. with $\Delta^{44/42}Ca_{bone\text{-}blood}$ between 0 and -0.1 ‰). Note that
432 considering the Ca residence time in bones (about 5 to 6 years for sows) and the length of
433 the experiment (less than 6 months), $\delta^{44/42}Ca$ values from sow bones collected at the end of
434 the experiment are considered to be minimally affected by gestation (3 months) and
435 lactation periods (28 days) experienced during the experiment. Instead, these bone $\delta^{44/42}Ca$
436 values are more comparable with pre-insemination body Ca isotopic compositions. This is
437 confirmed by bone data obtained from the individual C8 (the sow who died between the
438 previous breeding cycle and the monitored breeding cycle), which is identical to C1, C2 and
439 C3 bone $\delta^{44/42}Ca$ values.

440 In gestation condition (GestR), predictions for urine and fetus tissues fit well within the range
441 of experimental syn-gestation urine and syn-parturition umbilical blood compositions, for
442 steady state (i.e. post 10^4 days) as for 100-day simulations. Steady state and 100-days

443 $\delta^{44/42}$Ca values predicted for extracellular fluids are higher than experimental blood $\delta^{44/42}$Ca
444 range of the last month of gestation, by an order of 0.1 to 0.2 ‰. None of our experimental
445 bone $\delta^{44/42}$Ca values are comparable with 100 days or steady state gestation simulations,
446 however low $\alpha_{B\text{-}EF}$ (i.e. high enrichment in light Ca isotopes at bone mineralization) increases
447 the gap between predicted extracellular fluid $\delta^{44/42}$Ca values at 100 days (GestR) and the
448 range of experimental syn-gestation blood $\delta^{44/42}$Ca values (figure C.5).

449 Model predictions for urine, extracellular fluids and milk $\delta^{44/42}$Ca values for the high dairy
450 excretion scenario (LactA) are all higher than the range of experimental data obtained during
451 nursing for these fluids, for steady state as for 100-days simulations. As these fluids keep a
452 similar Ca isotopic composition between 2 and 100 days, we can postulate that 100-days
453 simulations are comparable with experimental data at 14 days of lactation (with moderate
454 reserves regarding the overlooking of non-secreting soft tissue dynamic in the model).
455 Model predictions within the low dairy excretion scenario (LactB) for extracellular fluids and
456 milk $\delta^{44/42}$Ca values (for steady state and for 100-days simulations) fall in the range of
457 experimental data for blood and milk obtained during nursing. For urine, only 100-days
458 simulations predict $\delta^{44/42}$Ca values, which are in the upper range of experimental urine
459 $\delta^{44/42}$Ca values during nursing.

460 Comparisons between lactation scenarios at 1000 days with various intensity of bone loss,
461 predict that bone loss and its intensity have a negligible impact on the state of the system at
462 1000 days (i.e. on the long term), and only strongly affects bone Ca isotopic composition
463 (figure C.6). This is the logical consequence of decreasing the bone Ca residence time by
464 decreasing the bone reservoir size through bone loss. The different configurations of Ca
465 digestive excretions we tested (i.e. K→Ur/EF→Fs ratios ranging from 0.5 to 2) show that this

parameter has a restricted impact on the evolution of the system, for steady state (figure C.7) as for intermediate isotopic compositions (under 10^4 days).

Simulations with lower Ca absorption through the digestive tract (figure 8) show that decreasing Ca absorption leads to lower $\delta^{44/42}Ca$ values for urine, feces and blood, and eventually bone after 100 days of simulation. By dividing Ca absorption by 4 compared to gestation conditions without Ca transfer to fetuses (GestFF), blood $\delta^{44/42}Ca$ values decrease by about -0.20 ‰ (figure 8). The predicted $\Delta^{44/42}Ca_{bone\text{-}diet}$ in such case is -0.46 ‰, which differs from the -0.26 ‰ predicted for regular GestFF conditions, and the -0.28 ‰ we observe experimentally.

4. Discussion

4.1. Urine isotopic stability and Rayleigh distillation process

Despite the fact that pre-insemination and post-weaning steps should be similar in terms of body Ca fluxes for the animals (both take place two weeks after weaning), the range of Ca concentrations reported in morning-first urines is about 2.5 wider at the pre-insemination step than during all the rest of the experiment (figure C.2). This suggests that Ca concentrations in these urines is quite uninformative of daily urinary Ca fluxes, probably because the water balance status of the animals is too variable between samplings. Urine collected with that procedure however highlights a decrease of blood to urine isotopic difference during lactation ($\Delta^{44/42}Ca_{urine\text{-}blood}$ change from $+1.39^{+0.11}_{-0.12}$ ‰ during gestation to $+0.90^{+0.11}_{-0.12}$ ‰ during nursing, figure 4), when sow generally increase their Ca urinary losses [33]. This is compatible with the effect of a Rayleigh distillation process, resulting in lower $\Delta^{44/42}Ca_{urine\text{-}blood}$ for higher Ca urinary excretions [3,22,28]. As no other factor influencing

488 $\Delta^{44/42}Ca_{urine\text{-}blood}$ has yet been described, this provides additional support that a Rayleigh
489 distillation process affects Ca isotopic fractionation within kidneys.

490 This Rayleigh distillation is also a possible explanation to why urine collected during nursing
491 displays a range of $\delta^{44/42}Ca$ values which is lower than what the model predicts (figure 7,
492 LactA and LactB). Indeed, in the model the $\Delta^{44/42}Ca_{urine\text{-}blood}$ offset is constant (equal to +1.15
493 ‰[3,17,21,23]) and does not change with Ca urinary fluxes such as expected with a Rayleigh
494 distillation process operating at Ca renal reabsorption. Taking a Rayleigh distillation process
495 into account would mechanically decrease $\Delta^{44/42}Ca_{urine\text{-}blood}$ for high Ca urinary excretions[3,22,28]
496 (e.g. during pig lactation[33]), and thus lower blood, urine, feces and milk $\delta^{44/42}Ca$ values
497 compared to predicted values in LactA and LactB simulations (figure 7). Alternatively, taking
498 into account a lower dairy Ca flux also reduces the mismatch between experimental and
499 model data (figure 7, LactB). However, if this last scenario is consistent with the lower range
500 of milk production and Ca dairy excretion we estimate (about 8.2 g of Ca per day, table B.5),
501 it seems partially incompatible with the range of Ca concentration classically reported in milk
502 (> 1500 mg/l [33,41] compared to a minimum of 817 mg/l for this study, table B.5). The Rayleigh
503 distillation hypothesis seems thus more parsimonious to explain the difference between
504 experimental and model data in lactation conditions.

505 Thus, our observations support that a Rayleigh distillation process operates during Ca renal
506 reabsorption, but also that comparing blood and urine Ca isotopic compositions (i.e.
507 $\Delta^{44/42}Ca_{urine\text{-}blood}$) collected by following our procedure (i.e. night of fasting, morning-first urine
508 and blood collection) can be used to detect changes in daily Ca urinary excretions without
509 having to collect 24h urines. As such, this method can help monitoring Ca retention in the

body and bone balance, which can be useful when 24h urine collections are difficult or impossible to set up (e.g. for studying large mammals other than humans).

4.2. Ca isotopic fractionation in pre-insemination conditions

In pre-insemination conditions, blood is depleted in heavy Ca isotopes relative to urine ($\Delta^{44/42}Ca_{urine\text{-}blood} = +1.17^{+0.11}_{-0.12}$ ‰, $n_{urine} = 3$, $n_{blood} = 3$; figure 3a), which is conform to the value of the literature ($\Delta^{44/42}Ca_{urine\text{-}blood} \approx +1.15$ ‰[3,17,21,23]), an isotopic fractionation generated by the preferential reabsorption of light Ca isotopes from primary urines to blood in kidneys[17,20–24,27]. The same blood samples, however, have an isotopic composition very similar to bones ($\Delta^{44/42}Ca_{bone\text{-}blood} = -0.08 \pm 0.11$ ‰, $n_{bone} = 3$, $n_{blood} = 3$; figure 3a), which suggest a low to null amplitude of isotopic fractionation between blood and bone during mineralization. This agrees with other observations of low blood-bone differences of Ca isotopic compositions in sheep, rats and humans[3,27] and predictions of quantitative modeling[3], but challenges previous hypotheses involving a $\Delta^{44/42}Ca_{bone\text{-}blood}$ of the order of -0.6 ‰ [2,5,6,14,17,21–23].

Similarly, the predictions of our model are only compatible with our experimental data when considering a small Ca isotopic fractionation at bone mineralization (i.e. $\Delta^{44/42}Ca_{bone\text{-}extracellular\ fluids}$ between 0 and -0.1 ‰; figure 7, GestFF). Along with other publications on the subject[3,27], this finding supports that the quantitative implications of kidney-mediated Ca isotopic fractionation on the body isotopic equilibrium could have been underestimated, and that, conversely, Ca isotopic fractionation at bone mineralization could be less pronounced than previously thought [2,3]. This mismatch between studies is likely favored by the wide diversity of Ca residence time in biological tissues and fluids that are compared. For example, it takes decades for bone to be at the isotopic steady state with blood (figure 6), whereas blood Ca isotopic composition can likely change in minutes to hours in response to transient

physiological states such as food consumption. Few hours of fasting (e.g. Heuser et al. 2016[17] and this study) likely limit the impact of these transitory events, but also provide data which are not fully representative of tissue and fluid Ca isotopic compositions over a day period. Thus, accurate direct comparisons are difficult outside of long-term feeding experiments (several years), whereas comparisons made in the literature are punctual in nature[2,5,6,14,17,21–23].

Nevertheless, apart from blood to bone differences, these two models of Ca isotopic fractionation (i.e. small versus large Ca isotopic fractionation at bone mineralization) can generate similar body Ca isotopic compositions despite their conceptual differences. For example, as long as bone resorption is associated with increased Ca urinary losses and bone accretion with decreased Ca urinary losses, both models stay compatible with the decrease of blood and urine $\delta^{44/42}$Ca values documented during bone loss events [6,20–23,28]. However, considering a smaller Ca isotopic fractionation at bone mineralization also provides new perspectives about some observations of the literature. For example, induced bone loss in Göttingen minipigs[17] is not associated with higher Ca urinary excretions or with a decrease of blood and urine $\delta^{44/42}$Ca values [17,42]. However, blood and urine $\delta^{44/42}$Ca values do decrease for humans with bone loss [20,24,28], while there are clues that bone loss comes with higher Ca urinary excretions for them (e.g. higher Ca concentrations in urines: Eisenhauer et al., 2019; Heuser et al., 2019)[20,28]. This suggests that bone losses can be efficiently monitored with Ca isotopes only when associated to increased urinary excretions, which is precisely the kind of difference predicted by the model we support in this study (i.e. $\Delta^{44/42}Ca_{bone\text{-}blood} < 0.3$ ‰, $\Delta^{44/42}Ca_{urine\text{-}blood} \approx +1.15$ ‰). Overall these results thus specify the range of physiological and pathological contexts where Ca isotopes can be used to monitor bone balance.

4.3. Ca isotopic fractionation from diet to bone during gestation

The difference between diet and bone Ca isotopic composition reported in this study ($\Delta^{44/42}Ca_{bone\text{-}diet}$ = -0.28 ± 0.11 ‰, n_{bone} = 3, n_{diet} = 3) is at odds with the relatively constant value generally reported among mammals (mean $\Delta^{44/42}Ca_{bone\text{-}diet}$ = -0.54 ± 0.08 ‰[2,3,5,9,13,17,27]). This study is among the first to report such a different and smaller $\Delta^{44/42}Ca_{bone\text{-}diet}$ value. To our knowledge, only Heuser et al. (2016)[17] previously described a similarly low $\Delta^{44/42}Ca_{bone\text{-}diet}$ value in Göttingen minipigs with glucocorticosteroid induced osteoporosis ($\Delta^{44/42}Ca_{bone\text{-}diet}$ = -0.32 ± 0.15 ‰)[17], although this result falls in the range of uncertainty reported in the literature[2,3,5,9,13,17,27]. This raises questions about the cause behind these differences. Simulations of gestation without Ca transfer to fetal tissues (GestFF) predicts the same isotopic compositions than what we observe experimentally and similarly generate a small $\Delta^{44/42}Ca_{bone\text{-}diet}$ (figure 7). This suggests that apparently no exotic parameter is needed to generate this small $\Delta^{44/42}Ca_{bone\text{-}diet}$. An important point is that the GestFF simulation involves Ca fluxes documented during gestation with the exception of fetal Ca transfer (table B.3). This is relevant as a general condition of the sows only because these domestic animals underwent repetitive gestations, representing more than two-third of their life time after their sexual maturity. In the wild, medium and large sized mammals generally experience bigger time gaps between gestations, with $\Delta^{44/42}Ca_{bone\text{-}diet}$ documented so far arising largely from wild animals, non-breeding animals or primiparous females [5,9,13,17]. This suggests that changes in Ca fluxes during gestation can change the bone-diet isotopic offset (i.e. $\Delta^{44/42}Ca_{bone\text{-}diet}$).

The study of sow Ca balance in normal adult condition (i.e. outside of the gestation and lactation periods) attracted little attention so far. However, we can reasonably assume that Ca absorption in the digestive track increases during gestation compared to normal

conditions, with gestation involving more Ca dietary intakes in order to adapt to higher Ca demands (see example for humans: Kovacs and Fuleihan, 2006)[43]. Dividing Ca absorptions by 4 (compared to GestFF conditions) changes predicted $\Delta^{44/42}Ca_{bone\text{-}diet}$ values from -0.26 ‰ to -0.46 ‰ (figure 8), which then falls within the range of the general $\Delta^{44/42}Ca_{bone\text{-}diet}$ documented for mammals (mean $\Delta^{44/42}Ca_{bone\text{-}diet}$ = -0.54 ± 0.08 ‰ [2,3,5,9,13,17,27]). This demonstration is purely conceptual as only Ca absorption, fecal Ca losses and the blood→waste Ca flux are modified from GestFF conditions in figure 8, whereas changing Ca absorption in a real organism would likely trigger other changes in Ca fluxes (e.g. urinary). Moreover, any modification of the ratio between Ca absorption and Ca urinary excretion fluxes can modify the $\Delta^{44/42}Ca_{bone\text{-}diet}$[3]. Monitoring an animal population with various Ca absorption levels (e.g. with different Ca content in the diet), would thus be necessary to precisely describe the effect of Ca absorption on body isotopic compositions. Nevertheless, there remains a strong suspicion that the small $\Delta^{44/42}Ca_{bone\text{-}diet}$ reported in this study could be the consequence of prolonged higher food Ca absorptions (with a lower Ca absorption/Ca urinary excretion ratio), notably caused by consecutive gestation periods. Furthermore, the reduction of the $\Delta^{44/42}Ca_{bone\text{-}diet}$ can also be further amplified by the repeated export of light Ca isotopes through placental and milk transfers (see sections 4.4. and 4.5.).

This consequence of frequent reproductions is important to consider for Ca isotope studies involving livestock animals, but likely plays a minor role in animal populations reproducing less intensively. Thus, we can reasonably assume that this gestation effect is only a minor issue for trophic studies of wild faunas involving Ca isotopes. First, because gestation decreases the $\Delta^{44/42}Ca_{bone\text{-}diet}$ values but does not cancel entirely the trophic level effect (TLE). Second, because this phenomenon will be active only for females with gestation periods

603 constituting the majority of their lifetime, a condition which is relevant only for a fraction of
604 females in specific mammal species and populations[44].

605 *4.4. Gestation effects on body $\delta^{44/42}Ca$ values*

606 As discussed in the previous section, gestation periods appear to be associated with smaller
607 $\Delta^{44/42}Ca_{blood\text{-}diet}$ and $\Delta^{44/42}Ca_{bone\text{-}diet}$ offsets, resulting in overall higher body $\delta^{44/42}Ca$ values than
608 what could be expected in normal conditions (figures 7 and 8). However, there is no major
609 change of urine and blood Ca isotopic compositions between pre-insemination and end-
610 gestation periods. We do observe a decrease of blood $\delta^{44/42}Ca$ values of about -0.2 ‰ for two
611 individuals (C1 and C2, figure 3c), but we suspect that this difference is a stochastic
612 underestimation of blood $\delta^{44/42}Ca$ inter-individual variability during the last month of
613 gestation. This phenomenon is likely because only 3 individuals have been monitored and
614 that blood $\delta^{44/42}Ca$ values from this period are by far the most homogenous of all sampling
615 steps (figure 3c). Alternatively, this could be explained by the fact that blood compositions
616 are not entirely free of nursing influence for C1 and C2 individuals at the pre-insemination
617 step, as it follows a previous weaning by only 12 to 14 days (similarly as the monitored post-
618 weaning step).

619 The fact that urines and blood $\delta^{44/42}Ca$ values remain stable, or decrease between pre-
620 insemination and end-gestation periods (figure 3), is at odds with modeling predictions
621 suggesting an increase of +0.10 to +0.15 ‰ (figure 7, difference between GestFF and GestR).
622 A possibility is that Ca isotopic fractionations between sow blood and fetal tissues are in
623 reality less pronounced than what is considered in GestR simulation (i.e. a $\Delta^{44/42}Ca_{umbilical\ blood\text{-}}$
624 $_{sow\ blood}$ closer to 0 ‰ than -0.18 ‰). At the moment, the data we obtained from sow blood
625 and umbilical blood at birth are the first direct data to document potential isotopic

626 fractionations associated with this flux. However, it is yet to be confirmed if the average
627 difference of -0.18 ± 0.11 ‰ we measure between these fluids (or -0.14 ± 0.11 ‰ for the
628 best temporal match) is representative of a full gestation period or only of birth. Several
629 independent clues suggest that the general $\Delta^{44/42}Ca_{\text{umbilical blood-sow blood}}$ offset could be closer to 0
630 ‰. For example, the individual C2 carried only 2 piglets against 16 and 18 piglets for C1 and
631 C3, which should result in Ca placental transfers that would be 5 to 6 times smaller for C2
632 (see total piglet Ca mass in Table B.5). However, despite this huge difference and the fact
633 that these Ca transfers should peak around the sampling period [45,46], body Ca isotopic
634 compositions of C2 do not exhibit an exotic pattern between pre-insemination and late
635 gestation periods compared to C1 and C3 (figure 3). Additionally, the two juveniles who died
636 at and closely after birth have bone Ca isotopic compositions undistinguishable from adults
637 (figure 2). A similar observation has been documented between human young infants and
638 adults who display low to absent difference between their bone Ca isotopic compositions [8].
639 This seems partly incompatible with the low $\delta^{44/42}Ca$ values recorded in human enamel
640 growing in utero [18,19], but could be explained if umbilical blood Ca is only significantly ^{44}Ca-
641 depleted during a relatively short period before birth, such as suggested by other human
642 enamel data [15]. If further investigations confirm that the general Ca isotopic fractionation
643 between gestating females and their fetuses is small, this would make gestation model
644 predictions (GestR) converge with gestation predictions without Ca placental transfer
645 predictions (GestFF), with the bulk fetus Ca isotopic composition being equal to sow
646 extracellular fluids in average (figure 7, GestFF). Nevertheless, the fact that Ca isotope body
647 compositions predicted for 100-days gestation simulations (GestR) remain in the range of
648 pre-insemination experimental $\delta^{44/42}Ca$ values (figure 7), emphasizes that even a Ca isotopic
649 fractionation factor of 0.99982 at Ca placental transfers from sow to fetuses (representative

of a $\Delta^{44/42}Ca_{umbilical\ blood\text{-}sow\ blood}$ = - 0.18 ‰) would have a restricted effect on sow body Ca isotopic compositions. Finally, contrary to what we consider in the model of this study (figure 5), Ca transfer does occur in reality from the umbilical reservoir to the sow blood reservoir [47]. We can suppose that this flux is associated with an isotopic fractionation factor equal to 1 or less (because this is generally what is observed for trans-membrane transport[3]). As such, this flux likely attenuates the effect of placental Ca transfers on sow body composition and further explains why we do not detect $\delta^{44/42}Ca$ differences between bones from newborn and adults, or between C2 $\delta^{44/42}Ca$ patterns and those of the other specimens.

These results also provide new insights about the higher bone $\delta^{44/42}Ca$ values (+0.14 ± 0.08 ‰) documented for ewes when compared to male sheep from the same herd [14]. With a model which is very different from that of this study, as it notably involves important Ca isotopic fractionation at bone mineralization and no renal fractionation, the authors pointed to bone accretion during gestation as one of the potential drivers of the sexual isotopic difference. Our data do not support this hypothesis, because we do not observe any marked increase in blood $\delta^{44/42}Ca$ values during gestation, while blood is expected to experience an even greater increase of $\delta^{44/42}Ca$ values than bone in such a scenario. This can be caused by the fact that sows did not experience bone accretion over the course of their gestation, but can be explained more generally because bone mineralization seems associated with a Ca isotopic fractionation factor closer to 1 than previously thought (see section 4.2. and [2,3]). Nevertheless, we demonstrated that gestation periods could increase body $\delta^{44/42}Ca$ values for other reasons than bone accretion (figure 8 and section 4.3.). To some extent, gestation periods are thus likely contributing to the higher bone $\delta^{44/42}Ca$ values documented in female sheep [14].

4.5. Control of lactation on body $\delta^{44/42}Ca$ values

Our experiment highlights a significant increase of adult blood $\delta^{44/42}Ca$ values during nursing compared to pre-parturition values ($\Delta^{44/42}Ca_{\text{nursing blood-gestation blood}} = +0.42^{+0.11}_{-0.12}$‰, figure 3c), joining similar observations done in mice [9]. Giesemann et al. (1998)[33] showed that besides milk production, lactation in sows was associated with bone resorption as well as higher Ca dietary absorption, digestibility and urinary excretions. Having higher Ca urinary losses during lactation is however not a constant among mammals. This is notably the opposite of what was documented for humans [43], and emphasizes why changes in $\Delta^{44/42}Ca_{\text{urine-blood}}$ (figure 4, discussed in section 4.1.) cannot be used as a universal lactation signal. Simulations highlight that higher Ca dietary absorption, urinary excretion and milk production conjointly increase blood $\delta^{44/42}Ca$ values during lactation (figure 7, 8, C.6, C.7), with milk production being the dominant factor of this isotopic change. As a flux, Ca dairy excretion exceeds Ca urinary excretions by two orders of magnitude (table B.5 and [33]) and constitutes by far the biggest change from normal or gestation conditions to lactation conditions. This flux comes with important Ca isotopic fractionation at milk production, as suggested by $\Delta^{44/42}Ca_{\text{milk-diet}}$ data (-0.6 ‰ [13]; -0.58 ± 0.12 ‰, this study) and $\Delta^{44/42}Ca_{\text{milk-blood}}$ data (-0.67 ± 0.12 ‰, this study), and therefore strongly affects blood and the whole body Ca isotopic compositions. This is particularly clear when comparing low versus high milk production simulations (LactA and LactB, figure 7). A decrease of about half the Ca dairy excretion (between LactA and LactB) results in a decrease of $\delta^{44/42}Ca$ values of the order of 0.25 ‰ in extracellular fluids (i.e. blood), urine and milk. The increase of $\delta^{44/42}Ca$ values in the maternal blood during nursing can therefore be described as a lactation signal which exceeds the effects of gestation. Nevertheless, the amount of milk produced per day and Ca dietary intakes also change a lot between species. This heterogeneity between mammal species could thus be an

698 important modulatory factor for the expression of this lactation signal among mammal
699 species.

700 *4.6. Lactation signal record within mineralized tissues*

701 In terms of rate, body Ca reservoirs are expected to react very rapidly after the onset of
702 lactation Ca fluxes, with the exception of bone (figure 6). In our experiment however, these
703 changes seem to appear only after a few days from parturition (e.g. 5 days for C3, figure 3c).
704 This minor inconsistency can be explained partly by the fact that our model neglects the Ca
705 storage in non-secreting organs and soft tissues, but also by the lower dairy Ca excretion
706 through colostrum and milk during the first days following parturition [48]. As for its onset, the
707 blood lactation signal we describe also attenuates rapidly (in few weeks) as the sow comes
708 back to normal physiological conditions. It seems to be the case 14 days after weaning, with
709 blood post-weaning $\delta^{44/42}$Ca values matching pre-insemination values (this is particularly
710 clear for the C3 individual, figure 3c), although we cannot guarantee that the pre-
711 insemination step was completely free of nursing influence (only 12 to 14 days separate this
712 step from the weaning of the previous litter). Preserving such a lactation signal within
713 mineralized tissues (i.e. bones and teeth) is thus only possible if the lactation is sustained for
714 enough time. For bones, the model predicts about 100 days before a significant change can
715 be recorded (figure 6) and a shorter time if bone loss is involved (figure C.6). A similar animal
716 with longer nursing period than sows would thus likely preserve a lactation signal within
717 bone, providing that it dies close enough from a lactation period to not attenuate the signal
718 too much with bone remodeling (in the model 50% of the Ca of bones is renewed after
719 about 3.8 years). Nevertheless, preserving such signal in teeth that would mineralize during
720 a lactation period is also possible for certain mammal species and would likely constitute an
721 even better record considering how enamel grows and preserves isotopic compositions [49].

As previously mentioned, is has been shown that modern ewes have higher bone $\delta^{44/42}Ca$ values than males within the same herd [14]. Besides bone accretion during gestation, the authors pointed to milk excretion as an alternative driver of this sexual isotopic difference. Our study supports that such signals can result from Ca flux changes during lactation, mainly because of the milk excretion, but also to a lesser extent because of the increase of dietary Ca intakes and urinary excretion during lactation and preceding gestation. The average $\Delta^{44/42}Ca_{females\text{-}males}$ reported in bones of ewes compared to male sheep (+0.14 ± 0.08 ‰)[14], falls within the range of what could be reasonably expected for pigs if they sustained a lactation over 1 year without undergoing bone loss (figure 6). Although this is longer than what ewes usually do and very far from sow typical nursing duration [50], lactation induced bone loss can increase the bone reactivity to lactation isotopic changes and likely helps recording such a lactation signal (figure C.6). Consecutive gestations and lactations, such as classically experienced by livestock animals, and a death relatively close from lactation, are also favorable factors to preserve such signals. This makes lactation a very suitable candidate to explain differences in bone Ca isotopic composition between sexes of adult mammal populations having a similar diet, such as observed for modern ewes [14]. Besides, this provides an additional explanation to why human populations studied so far do not exhibit such differences [8,14]. Obviously the predictions of our model cannot be directly applied to sheep, as many Ca fluxes and reservoir sizes change between sow and sheep in addition to the length of lactation of these animals. However, our model and experimental data provide the basics and order of magnitude of what could be expected in other medium to large mammal species. Considering all of that, preserving this lactation signature within bones or teeth of other mammal species, including extinct ones, seems plausible. This would allow studying past lactation habits using bone or teeth Ca isotopic compositions, but could

concurrently complicate the use of Ca isotopes as a trophic indicator. However, our study suggests the timings and lengths of lactation periods necessary to preserve such a lactation signal likely concern a fraction of mammal species only[44]. Additionally, the sheep population studied by Reynard et al. (2010)[14] suggests that this signature of the lactation tends to stay of small amplitude (+0.14 ± 0.08 ‰)[14], despite the fact that females from this population went through 3 consecutive gestations and lactations in that study. Thus, the effects of lactation we describe here do not seem to be a major issue for using Ca isotopes as a trophic indicator, especially when studying wild faunas.

5. Conclusion

Through modeling and a longitudinal monitoring of a sow population, this study provides new insights about the mammalian isotopic Ca cycle. Our data support a model of Ca isotopic fractionation with a less pronounced fractionation during bone mineralization than previously proposed ($\Delta^{44/42}Ca_{bone\text{-}blood}$ below -0.3 ‰ instead of about -0.6 ‰), a change which specifies the range of physiological and pathological contexts where Ca isotopes can be used to monitor bone balance. Although of small amplitude and apparently not representative of the full length of the gestation, we detected that umbilical blood is ^{44}Ca-depleted compared to maternal blood ($\Delta^{44/42}Ca_{umbilical\ blood\text{-}\ sow\ blood}$ = -0.18 ± 0.11 ‰, n = 3; or -0.14 ± 0.11 ‰ for the best temporal match). Apart from this fractionation, gestation seems to be associated with overall higher body $\delta^{44/42}$Ca values and lower isotopic differences between diet and bones than for other mammals in normal physiological conditions ($\Delta^{44/42}Ca_{bone\text{-}diet}$ = -0.28 ± 0.11 ‰), possibly because of higher Ca absorptions by the digestive track. Lactation periods are associated with even higher blood $\delta^{44/42}$Ca values ($\delta^{44/42}Ca_{blood}$ change of $+0.42^{+0.11}_{-0.12}$ ‰ during nursing) and with small isotopic differences between urine and blood ($\Delta^{44/42}Ca_{urine\text{-}blood}$ =

769 $+0.90^{+0.11}_{-0.12}$‰), although this last observation is likely a less universal lactation marker. The
770 high blood $\delta^{44/42}$Ca values are mainly caused by milk production and excretion, and are likely
771 the main cause of male versus female differences in bone Ca isotopic composition
772 documented in certain mammal populations. According to our model, the preservation of
773 such lactation events in bone is favored by greater Ca dairy excretions, by longer lactation
774 periods, by smaller time gaps between nursing periods, as well as by a death or bone
775 sampling close to the lactation period.

776 **6. Acknowledgements**

777 We thank Yoann Bailly, Stéphane Moreau, Tony Terrasson and the rest of the team of
778 GENESI for their dedicated investment in the project regarding animal management and
779 samplings. For technical assistance on spectrometers, we thank F. Arnaud Godet and P.
780 Telouk. We thank Gildas Merceron for organizing the meeting, which planted the seeds of
781 this project as well as many others. The authors are grateful to all the institutions which
782 supported the project.

783 **7. Funding sources**

784 This study was supported by the Interrvie program of INSU, CNRS (to JEM), by INRAE
785 (previously INRA) and by ENS de Lyon.

786 **8. Data Availability Statements**

787 The data underlying this article are available in the article and in its online supplementary
788 material. The Isopybox program used for building box model simulations and its resources
789 are accessible on Github at the following address: https://github.com/ttacail/isopybox.git.

9. Bibliography

1 J. E. Martin, T. Tacail and V. Balter, *Palaeontology*, 2017, **60**, 485–502.

2 T. Tacail, S. Le Houedec and J. L. Skulan, *Chem. Geol.*, 2020, **537**, 119471.

3 T. Tacail, PhD thesis. Université de Lyon, 2017.

4 Q. Li, M. Thirlwall and W. Müller, *Chem. Geol.*, 2016, **422**, 1–12.

5 J. Skulan and D. J. DePaolo, *Proc. Natl. Acad. Sci. U.S.A.*, 1999, **96**, 13709–13713.

6 J. Skulan, T. Bullen, A. D. Anbar, J. E. Puzas, L. S. Ford, A. LeBlanc and S. M. Smith, *Clin. Chem.*, 2007, **53**, 1155–1158.

7 A. D. Melin, B. E. Crowley, S. T. Brown, P. V. Wheatley, G. L. Moritz, F. T. Yit Yu, H. Bernard, D. J. DePaolo, A. D. Jacobson and N. J. Dominy, *Am. J. Phys. Anthropol.*, 2014, **154**, 633–643.

8 L. M. Reynard, J. A. Pearson, G. M. Henderson and R. E. M. Hedges, *Archaeometry*, 2013, **55**, 946–957.

9 T. Hirata, M. Tanoshima, A. Suga, Y. Tanaka, Y. Nagata, A. Shinohara and M. Chiba, *Anal. Sci.*, 2008, **24**, 1501–1507.

10 J. E. Martin, T. Tacail, T. E. Cerling and V. Balter, *Earth Planet. Sci. Lett.*, 2018, **503**, 227–235.

11 M. T. Clementz, P. Holden and P. L. Koch, *Int. J. Osteoarchaeol.*, 2003, **13**, 29–36.

12 M. T. Clementz, *J. Mammal.*, 2012, **93**, 368–380.

13 N. C. Chu, G. M. Henderson, N. S. Belshaw and R. E. M. Hedges, *Appl. Geochem.*, 2006, **21**, 1656–1667.

14 L. M. Reynard, G. M. Henderson and R. E. M. Hedges, *Geochim. Cosmochim. Acta*, 2010, **74**, 3735–3750.

15 Q. Li, A. Nava, L. M. Reynard, M. Thirlwall, L. Bondioli and W. Müller, *Environ. Archaeol.*, 2020, 1–10.

16 J. E. Martin, T. Tacail, S. Adnet, C. Girard and V. Balter, *Chem. Geol.*, 2015, **415**, 118–125.

17 A. Heuser, A. Eisenhauer, K. E. Scholz-Ahrens and J. Schrezenmeir, *Isotopes Environ. Health Stud.*, 2016, **52**, 633–648.

18 T. Tacail, B. Thivichon-Prince, J. E. Martin, C. Charles, L. Viriot and V. Balter, *Proc. Natl. Acad. Sci. U.S.A.*, 2017, **114**, 6268–6273.

19 T. Tacail, J. E. Martin, F. Arnaud-Godet, J. F. Thackeray, T. E. Cerling, J. Braga and V. Balter, *Sci. Adv.*, 2019, **5**, eaax3250.

20 A. Eisenhauer, M. Müller, A. Heuser, A. Kolevica, C. C. Glüer, M. Both, C. Laue, U. V. Hehn, S. Kloth, R. Shroff and J. Schrezenmeir, *Bone Reports*, 2019, **10**, 100200.

21 J. L. L. Morgan, J. L. Skulan, G. W. Gordon, S. J. Romaniello, S. M. Smith and A. D. Anbar, *Proc. Natl. Acad. Sci. U.S.A.*, 2012, **109**, 9989–9994.

22 A. Heuser and A. Eisenhauer, *Bone*, 2010, **46**, 889–896.

23 M. B. Channon, G. W. Gordon, J. L. L. Morgan, J. L. Skulan, S. M. Smith and A. D. Anbar, *Bone*, 2015, **77**, 69–74.

24 R. Shroff, M. Fewtrell, A. Heuser, A. Kolevica, A. Lalayiannis, L. Mcalister, S. Silva, N. Goodman, C. P. Schmitt, L. Biassoni, A. Rahn, D.-C. Fischer and A. Eisenhauer, *J. Bone*

Miner. Res., , DOI:10.1002/jbmr.4158.

25 A. Hassler, J. E. Martin, R. Amiot, T. Tacail, F. A. Godet, R. Allain and V. Balter, *Proc. R. Soc. B Biol. Sci.*, 2018, **285**, 20180197.

26 J. E. Martin, T. Tacail, J. Braga, T. E. Cerling and V. Balter, *Nat. Commun.*, 2020, **11**, 3587.

27 T. Tacail, E. Albalat, P. Télouk and V. Balter, *J. Anal. At. Spectrom.*, 2014, **29**, 529.

28 A. Heuser, P. Frings-Meuthen, J. Rittweger and S. J. G. Galer, *Front. Physiol.*, 2019, **10**, 12.

29 M. Peacock, *Clin. J. Am. Soc. Nephrol.*, 2010, **5**, 23–30.

30 A. H. Doherty, C. K. Ghalambor and S. W. Donahue, *Physiology*, 2015, **30**, 17–29.

31 M. C. Peterson and M. M. Riggs, *Bone*, 2010, **46**, 49–63.

32 J.-Y. Dourmad, M. Etienne, J. Noblet and D. Causeur, *Journées la Rech. Porc. en Fr.*, 1997, **29**, 255–262.

33 M. A. Giesemann, A. J. Lewis, P. S. Miller and M. P. Akhter, *J. Anim. Sci.*, 1998, **76**, 796–807.

34 M. Etienne, C. Legault, J.-Y. Dourmad and J. Noblet, *Journées la Rech. Porc. en Fr.*, 2000, **32**, 253–264.

35 F. Klobasa, E. Werhahn and J. E. Butler, *J. Anim. Sci.*, 1987, **64**, 1458–1466.

36 S. Le Goff, E. Albalat, A. Dosseto, J. Godin and V. Balter, *Rapid Commun. Mass Spectrom.*, , DOI:10.1002/rcm.9074.

37 C. N. Marechal, P. Telouk and F. Albarede, *Chem. Geol.*, 1999, **156**, 251–273.

38 T. Tacail, P. Télouk and V. Balter, *J. Anal. At. Spectrom.*, 2016, **31**, 152–162.

39 A. Heuser and A. Eisenhauer, *Geostand. Geoanalytical Res.*, 2008, **32**, 311–315.

40 K. Jaouen, L. Pouilloux, V. Balter, M. L. Pons, J. J. Hublin and F. Albarède, *Metallomics*, 2019, **11**, 1049–1059.

41 J. Novotný, P. Reichel, B. Kósa and D. Šipoš, *Folia Vet.*, 2018, **60**, 61–65.

42 K. E. Scholz-Ahrens, G. Delling, B. Stampa, A. Helfenstein, H. J. Hahne, Y. Açil, W. Timm, R. Barkmann, J. Hassenpflug, J. Schrezenmeir and C. C. Glüer, *Am. J. Physiol. - Endocrinol. Metab.*, 2007, **293**, E385–E395.

43 C. S. Kovacs and G. E. Fuleihan, *Endocrinol. Metab. Clin.*, 2006, **35**, 21–51.

44 K. E. Jones, J. Bielby, M. Cardillo, S. A. Fritz, J. O'Dell, C. D. L. Orme, K. Safi, W. Sechrest, E. H. Boakes, C. Carbone, C. Connolly, M. J. Cutts, J. K. Foster, R. Grenyer, C. A. Plaster, S. A. Price, E. A. Rigby, J. Rist, A. Teacher, O. R. P. Bininda-Emonds, J. L. Gittleman, G. M. Mace and A. Purvis, *Ecology*, 2009, 90:2648.

45 S. L. Hansard, H. Itoh, J. C. Glenn and D. M. Thrasher, *J. Nutr.*, 1966, **89**, 335–340.

46 H. Itoh, S. L. Hansard, J. C. Glenn, F. H. Hoskins and D. M. Thrasher, *J. Anim. Sci.*, 1967, **26**, 335–340.

47 J. Štulc, *Physiol. Rev.*, 1997, **77**, 805–836.

48 D. R. Perrin, *J. Dairy Res.*, 1955, **22**, 103–107.

49 R. B. Trayler and M. J. Kohn, *Geochim. Cosmochim. Acta*, 2017, **198**, 32–47.

872 50 K. Bøe, *Appl. Anim. Behav. Sci.*, 1991, **30**, 47–59.

873 51 L. Sauzéat, M. Costas-Rodríguez, E. Albalat, N. Mattielli, F. Vanhaecke and V. Balter,
874 *Talanta*, 2021, **221**, 121576.

875 52 K. V. Sullivan, Queen's University Kingston, Kingston, Ontario, Canada, 2020.

876 53 K. Sullivan, D. Layton-matthews, M. Leybourne, J. Kidder, Z. Mester and L. Yang,
877 *Geostand. Geoanalytical Res.*, 2020, **44**, 349–362.

878 54 Joint Committee for Guides in Metrology, *JCGM*, 2008, **100**, 116.

879 55 M. Horsky, J. Irrgeher and T. Prohaska, *Anal. Bioanal. Chem.*, 2016, **408**, 351–367.

880 56 A. Heuser, T. Tütken, N. Gussone and S. J. G. Galer, *Geochim. Cosmochim. Acta*, 2011,
881 **75**, 3419–3433.

882 57 T. Tacail, J. E. Martin, E. Herrscher, E. Albalat, C. Verna, F. Ramirez-rozzi, G. Clark and
883 V. Balter, *Quat. Sci. Rev.*, 2021, **256**, 106843.

884 58 C. Karlsson, K. J. Obrant and M. Karlsson, *Osteoporos. Int.*, 2001, **12**, 828–834.

885 59 D. M. Anderson, I. McDonald and F. W. H. Elsley, *J. Agric. Sci.*, 1969, **73**, 501–505.

886 60 D. C. Mahan and A. W. Fetter, *J. Anim. Sci.*, 1982, **54**, 285–291.

887 61 Z. Mroz, A. W. Jongbloed, N. P. Lenis and K. Vreman, *Nutr. Res. Rev.*, 1995, **8**, 137–
888 164.

889 62 J. Blaine, M. Chonchol and M. Levi, *Clin. J. Am. Soc. Nephrol.*, 2015, **10**, 1257–1272.

890 63 S. Luis-Lima, C. García-Contreras, M. Vázquez-Gómez, S. Astiz, F. Carrara, F. Gaspari, N.
891 Negrín-Mena, A. Jiménez-Sosa, H. Jiménez-Hernández, A. González-Bulnes and E.

892 Porrini, *Int. J. Mol. Sci.*, 2018, **19**, 1–12.

893 64 K. L. Penniston, S. R. Patel, D. J. Schwahn and S. Y. Nakada, *Urolithiasis*, 2017, **45**, 109–
894 125.

895

896 **10. Figures and tables**

897 *Figure 1. Sampling time chart*

898 Key steps and periods within the reproduction cycle of monitored specimens are
899 represented at the top of the figure. Sampling operations have been essentially conducted
900 during five key periods represented as dashed red area in the time chart and delimited by
901 dashed lines. Starting and ending dates of these periods are indicated at the bottom of the
902 time chart. From left to right these periods are representing: pre-insemination conditions,
903 the last month of gestation, the post-parturition period, nursing and post-weaning
904 conditions. Each sampling which lead to a $\delta^{44/42}Ca$ measure is represented by a colored bar.

905 *Figure 2. Fluid and tissue Ca isotopic compositions*

906 Ca isotopic compositions of all tissues and fluids collected from C1, C2, C3 and juvenile
907 individuals, expressed in ‰ as $\delta^{44/42}Ca_{ICP\ Ca\ Lyon}$ and $\delta^{44/42}Ca_{SRM915a}$ values. In these boxplots, the
908 central line represents the median, boxes are limited by their 1st and 3rd quartiles, and
909 whiskers extend to maximum and minimum values ± the uncertainties. The light green
910 shaded area represent the range of Ca isotopic composition of the diet with the mean
911 identified by the dashed line.

912 *Figure 3. Ca isotopic compositions over time*

913 Ca isotopic compositions of all samples collected from C1, C2 and C3, expressed in ‰ as
914 $\delta^{44/42}Ca_{ICP\ Ca\ Lyon}$ and $\delta^{44/42}Ca_{SRM915a}$ values over time. (a) All tissue and fluid Ca isotopic

915 compositions, (b) urine focus, (c) blood focus. Arrows, dashed black lines and associated P
916 and W marks on the x temporal axis respectively highlight parturition and weaning dates.
917 The size of the C2 colostrum data point is increased to make it visible despite the
918 superposition with the C2 umbilical blood data point. Error bars represent the range of
919 uncertainty around each value.

920 *Figure 4. Temporal evolution of $\Delta^{44/42}Ca_{blood}$ values*

921 Summary of $\Delta^{44/42}Ca_{X\text{-}blood}$ values (i.e. the difference between blood and other sample $\delta^{44/42}Ca$
922 values). For each individual, sample Ca isotopic compositions have been compared with
923 blood Ca isotopic compositions of the same sampling step, with the exception of bones
924 which are compared with pre-insemination blood $\delta^{44/42}Ca$ values. The shaded orange area
925 covers the range of urine $\Delta^{44/42}Ca_{X\text{-}blood}$ values ± the error bars. The orange line represents the
926 moving average of $\Delta^{44/42}Ca_{X\text{-}blood}$ values calculated for each sampling step. The size of the C2
927 colostrum data point is increased to make it visible despite the superposition with the C2
928 umbilical blood data point.

929 *Figure 5. Model of Ca cycle*

930 Box model of Ca body cycle adapted from the human model proposed by Tacail, 2017[3]. The
931 purple arrow and box are implemented to the model for gestation runs. The blue arrow and
932 box are implemented to the model for lactation runs. Yellow arrows represent Ca fluxes
933 going to the waste box, a theoretical reservoir of virtually infinite size which prevents Ca
934 output fluxes to interact with the rest of the system. The dashed yellow arrow is a
935 conceptual flux associated with no isotopic fractionation, notably used to nullify the growth
936 of the sow-like animal (see section 2.6.). The $\Delta^{44/42}Ca$ values considered in the model are
937 specified along their flux (hypotheses behind these values are specified in table B.4)

938 *Figure 6. Model evolution to steady state*

939 Evolution of Ca isotopic composition of sow Ca reservoirs in general conditions (GestFF),
940 gestating conditions (GestR), and lactating condition with higher or lower dairy Ca excretion
941 (LactA and LactB, repesctively). The x axis represents the time in days. These graphs
942 represent scenarios with no Ca isotopic fractionation at bone mineralization (i.e $\alpha_{B\text{-}EF}$ = 1),
943 however only bone Ca isotopic composition is notably affected by this fractionation factor.
944 Initial conditions of these simulations are summarized in tables B.2, B.3, B.4 and further
945 detailed in section 3.3.

946 *Figure 7. Model and experimental data comparison*

947 Comparison of modeling and experimental data in general condition (GestFF), gestating
948 condition (GestR), and lactating conditions with higher or lower dairy Ca excretion (LactA
949 and LactB, respectively). Points represent simulation results whereas colored zones
950 represent the range of $\delta^{44/42}$Ca values measured during our experiment at comparable stage
951 of the reproductive cycle. Simulation results are presented at day 100 and after 1000 days
952 when the sow system is in steady state (noted std*). Steady state simulations presented
953 here consider different Ca isotopic fractionation factor at bone mineralization (i.e. $\alpha_{B\text{-}EF}$
954 between 1 and 0.9994), representing a $\Delta^{44/42}Ca_{bone\text{-}blood}$ offset between 0 and 0.6 ‰ (only
955 bone is affected by this value). Bone data points tend toward red colors for $\alpha_{B\text{-}EF}$ = 1 (i.e. no
956 Ca isotopic fractionation at bone mineralization) and light blue colors for $\alpha_{B\text{-}EF}$ = 0.9994, with
957 0.0001 of difference between each neighbor color level. GestFF results are compared with
958 pre-inseminations $\delta^{44/42}$Ca values for urine and blood and with post-weaning $\delta^{44/42}$Ca values
959 for bones (see section 3.3.). GestR $\delta^{44/42}$Ca values are compared with late gestation urine,
960 sow blood and umbilical blood $\delta^{44/42}$Ca values at parturition. LactA and LactB are compared
961 with urine, blood and milk $\delta^{44/42}$Ca values from the nursing period. Bone $\delta^{44/42}$Ca values are

not displayed for 100 day simulations, because at this time bone are not yet significantly affected by changes in body Ca isotopic composition (see figure 6).

Figure 8. Ca absorption effect on body $\delta^{44/42}Ca$ values

Body Ca isotopic compositions predicted by our model at steady state in general condition (GestFF), with various Ca isotopic fractionation factor during bone mineralization (i.e. $\alpha_{B\text{-}EF}$), and various Ca absorption levels in the digestive track. Bone $\delta^{44/42}Ca$ predicted values are confounded with extra cellular fluids values for $\alpha_{B\text{-}EF}$ = 1 (i.e. no Ca isotopic fractionation at bone mineralization), and tend toward light blue colors for $\alpha_{B\text{-}EF}$ = 0.9994, with 0.0001 of difference between each neighbor color level. Absorption levels presented on the x axis range from 100% (left) to 25% (right) of Ca absorptions described by Giesemann et al. (1998) during gestation (table B.3). The grey shaded area represents the range of food $\delta^{44/42}Ca$ values from our experiment (uncertainties included), while the black line represents the average food $\delta^{44/42}Ca$ value. The green shaded area represents the range of bone $\delta^{44/42}Ca$ values expected with a mean $\Delta^{44/42}Ca_{bone\text{-}diet}$ of -0.54 ± 0.08 ‰[2,3,5,9,13,17,27].

11. Appendix A - Supplementary text

Text A.1 - Labware, consumables and cleaning procedures

This section provides additional details about the equipment used for this study as well as cleaning procedures performed before its use.

Text A.2 – Uncertainty of Ca isotopic compositions

This section describes in details how uncertainties presented in this study are calculated.

Text A.3 - Box model conception

This section describes with more details the conception of box-model simulations discussed in this paper.

12. Appendix B - Supplementary tables

Table B.1 - Chromatography

Three column chromatography procedure. This procedure is adapted from the methods of Tacail et al. (2014)[27] and Le Goff et al. (2021)[36].

Table B.2 - Model input (Initial reservoir sizes)

Reservoir sizes are expressed in mg of Ca and estimated from the following references [3,27,32,59–61].

Table B.3 - Model input (Ca fluxes)

Ca fluxes are described for the following simulations: GestFF, GestR, LactA, LactB, LactL, LactH and for GestFF with 75 % less Ca absorption in the digestive track. The bulk of these estimation are retrieved from Giesemann et al. (1998)[33], completed and compared with data from the present study and the following references [3,32,34,35,58,62–64].

Table B.4 - Model input (Ca isotopic fractionation)

We considered 6 Ca isotopic fractionation process in our model, based on data from this study and the literature [2,3,5,13,14,17,21–23,27].

Table B.5 - Zootechnical data

This table outline important zootechnical data collected from our experiment, such as the number of piglet per sow, weight and milk production estimations.

Table B.6 - Isotopic and elemental concentration data

This table synthetize all the data of Ca isotopic composition and elemental concentrations collected in this study, respectively expressed in ‰ and mg/kg of lyophilized sample (or mg/l for urine samples). In accordance with the data reported in appendix of Martin et al. (2018)[10] the uncertainties around $\delta^{44/42}Ca_{SRM\ 915a}$ values reported in this table are equal to the sum

between $\delta^{44/42}Ca_{ICP\ Ca\ Lyon}$ uncertainties and 0.025 ‰, the uncertainty around the $\delta^{44/42}Ca$ value of SRM915a measured against the ICP Ca Lyon. Sampling step labels correspond to periods at pre-insemination (AvIA), last month of gestation (G3), parturition (MB), nursing (M14) and post-weaning (S14).

13. Appendix C - Supplementary figures

Figure C.0 – SRM bootstrapping and baseline uncertainties

This figure synthetizes the results of different random samplings with replacement performed in the dataset of SRM1486 $\delta^{44/42}Ca$ values collected for this study. For each graphs, this random sampling collected a number n* of values (3, 4, 6 or 10) within the SRM1486 dataset constituted by 37 original values. A mean is calculated for each sampling of n* values and the procedure is repeated 100 000 times for each n* level. The difference between these means and the true mean of the dataset is calculated and the distribution of the results is presented within the graphs (in absolute value). Green zones represent 95 % of the means from the bootstrapping that were the closest from the true mean, red zones represent the 0.1 % of the means from the bootstrapping that were the most different from the true mean, blue zones represent intermediate values. For n* = 3 (i.e. three sampling with replacement), a number quite representative of the number of replicates for the $\delta^{44/42}Ca$ measures of samples from this study, 95 % of means from the bootstrapping fall within a ± 0.05 ‰ range around the true mean of the SRM1486 dataset. We designated this value as a minimum uncertainty around sample $\delta^{44/42}Ca$ measures.

Figure C.1 - Three isotopes plot

In this figure $\delta^{43/42}Ca$ values are plotted as a function of $\delta^{44/42}Ca$ values (‰, ICP Ca Lyon) for all samples and reference materials of this study, in black and green respectively. Ca isotopic

compositions fall on a line with a y-axis intercept of -0.003 ± 0.005 ‰ (2 standard errors), indistinguishable from theoretical 0 ‰ intercept. The slope value of this line is 0.502 ± 0.007 (2 standard errors), virtually identical to the 0.507 slope predicted by the exponential mass-dependent fractionation law. The two most external blue lines delimit the prediction interval, whereas the two red lines correspond to the 95 % confidence interval of the regression line. The regression line is represented in blue and is assimilated with the black dashed line representing the theoretical function (visible at the bottom left of the graph). The average 2 standard errors for $\delta^{43/42}Ca$ and $\delta^{44/42}Ca$ values is represented as a blue cross at the bottom right of the graph.

Figure C.2 - Ca concentration variability over time

(a) Evolution of Ca concentrations in morning urines over the experiment period. (b) Evolution of Ca concentrations in blood dry fraction over the experiment period. These concentrations are expressed in mg of Ca per kg of urine and lyophilized blood, respectively.

Figure C.3 - Correlation between Ca concentration and isotopic composition

(a) Logarithmic correlation between urine Ca isotopic compositions and urine Ca concentrations (R^2 = 0.37, p-value = 0.04). (b) Linear correlation between urine Ca isotopic compositions and urine Ca concentrations (R^2 = 0.35, p-value = 0.04). (c) Linear correlation between Ca isotopic compositions and Ca concentrations in blood dry fraction (R^2 < 0.01, p-value = 0.89).

Figure C.4 - $\Delta^{44/42}Ca_{X\text{-}blood}$ summary

The graph summarizes the data $\Delta^{44/42}Ca_{X\text{-}blood}$ collected in this study. For each individual, sample Ca isotopic compositions have been compared with blood Ca isotopic compositions

of the same sampling step, with the exception of bones which are compared with pre-insemination blood $\delta^{44/42}Ca$ values.

Figure C.5 - 100-day gestation and lactation simulations with variable $\alpha_{B\text{-}EF}$

Body Ca isotopic compositions predicted by our model at 100 days in gestation condition (GestR), and lactation conditions with higher or lower milk Ca output (LactA and LactB respectively). For each of these conditions, we simulated various degree of Ca isotopic fractionation at bone mineralization (i.e. $\alpha_{B\text{-}EF}$ include between 1 and 0.9994), representing $\Delta^{44/42}Ca_{bone\text{-}blood}$ offsets between 0 and 0.6 ‰. Colored areas represent the range of experimental data for urine (yellow), blood (red), fetal tissues (purple) and milk (blue). GestR $\delta^{44/42}Ca$ values are compared with late gestation urine, sow blood and syn-parturition umbilical blood $\delta^{44/42}Ca$ values. LactA and LactB are compared with urine, blood and milk $\delta^{44/42}Ca$ values from the nursing period.

Figure C.6 - 1000-day lactation simulations with variable $\alpha_{B\text{-}EF}$ and degree of bone loss

Body Ca isotopic compositions predicted by our model at 1000 days in lactation conditions without bone loss (LactA), with moderate bone loss (LactL) or important bone loss (LactH). For each of these situations, we simulated various degree of Ca isotopic fractionation at bone mineralization (i.e. $\alpha_{B\text{-}EF}$ include between 1 and 0.9994), representing $\Delta^{44/42}Ca_{bone\text{-}blood}$ offsets between 0 and 0.6 ‰.

Figure C.7 - steady state simulations with variable K→Ur/EF→Fs ratio

Body Ca isotopic compositions predicted by our model at steady state (for the sow) in normal condition (GestFF), gestation condition (GestR) and lactation condition (LactA). These simulations are done with a $\alpha_{B\text{-}EF}$ of 1 and variable ratio of urinary versus endogenous Ca

losses (i.e. K‣Ur / EF‣Fs), from 0.5 to 2. We changed this ratio by modifying Ca endogenous losses while keeping Ca urinary losses constant.

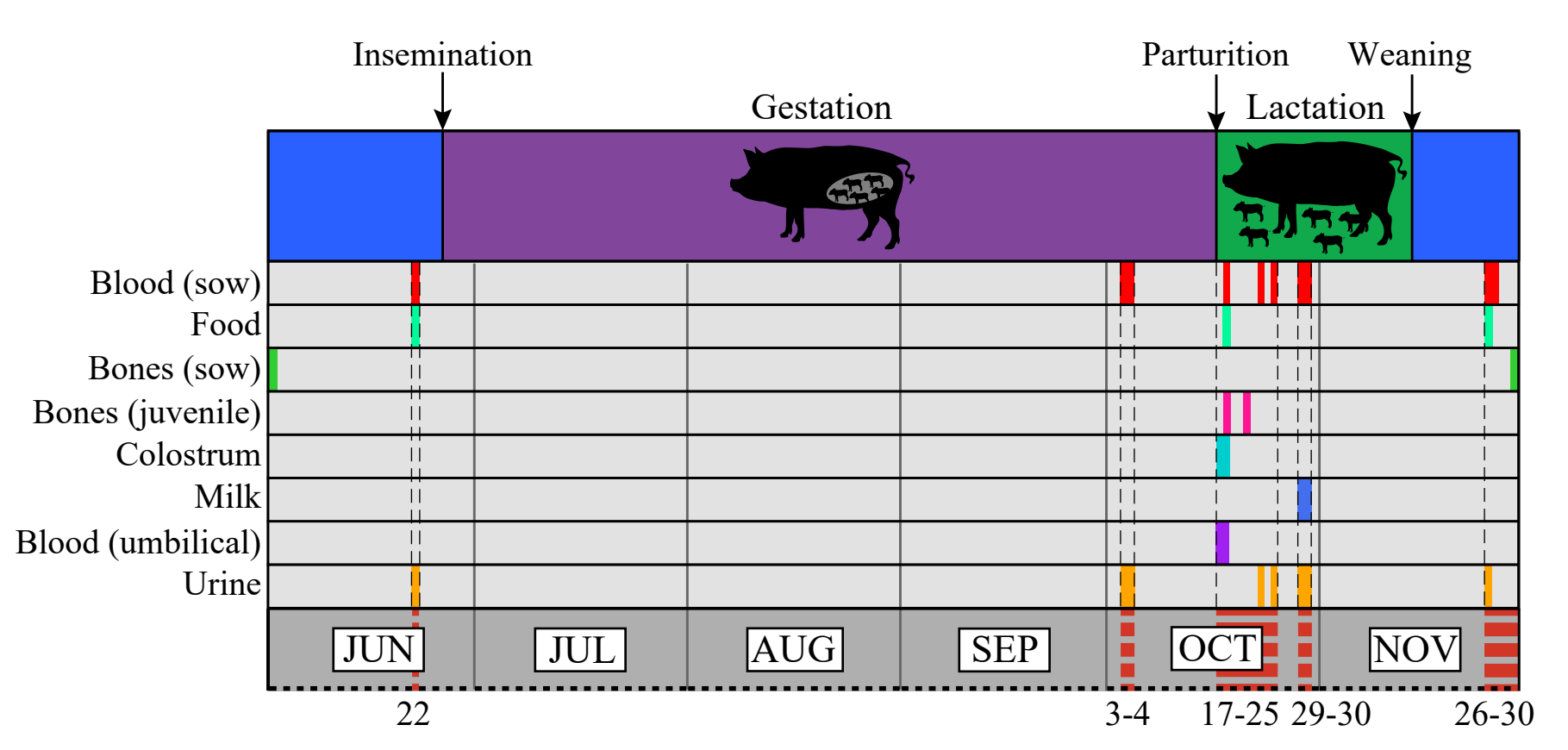
Insemination
Parturition
Weaning
Gestation
Lactation
Blood (sow)
Food
Bones (sow)
Bones (juvenile)
Colostrum
Milk
Blood (umbilical)
Urine
JUN
JUL
AUG
SEP
OCT
NOV
22
3-4
17-25
29-30
26-30

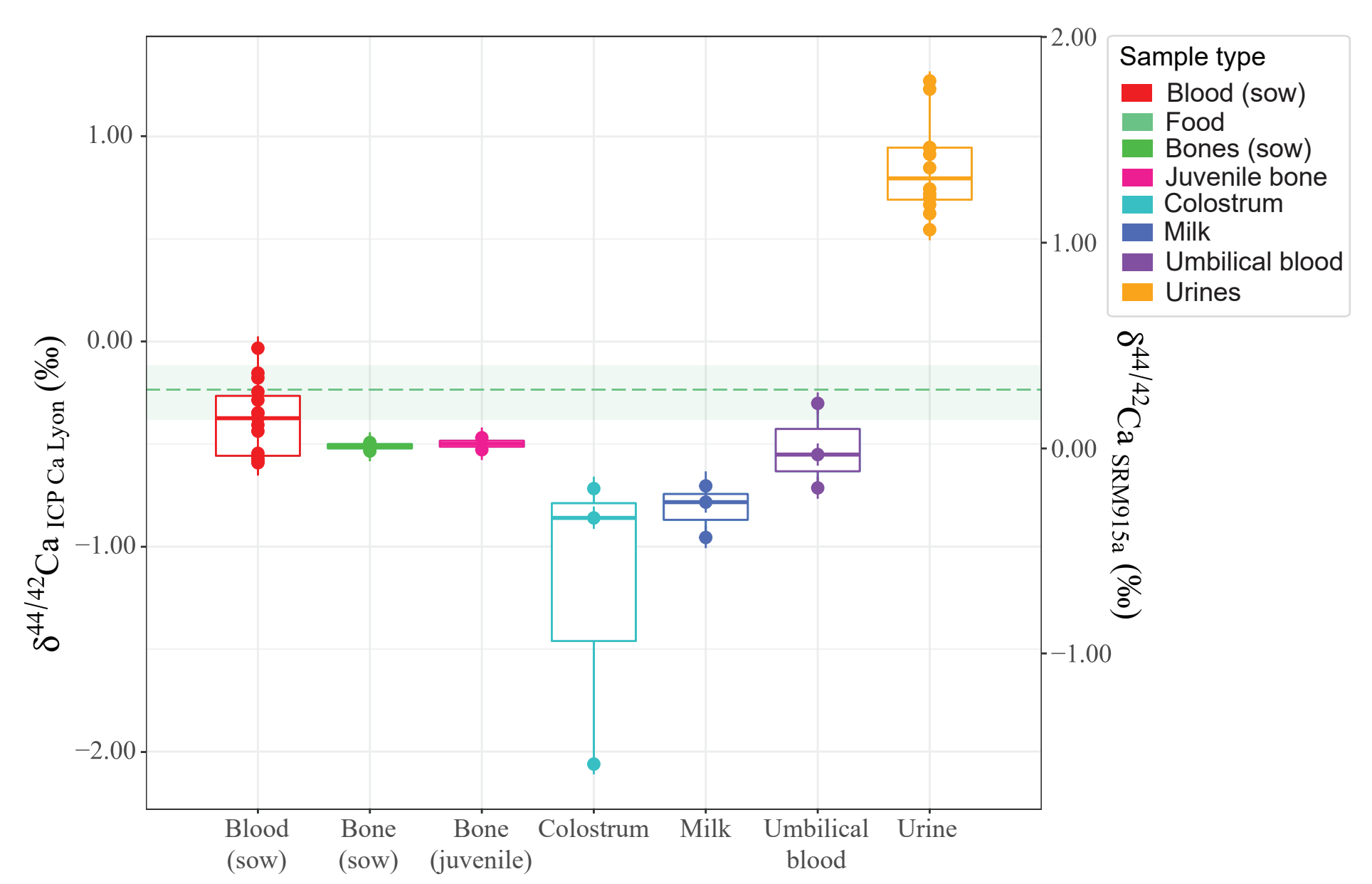
Sample type
Blood (sow)
Food
Bones (sow)
Juvenile bone
Colostrum
Milk
Umbilical blood
Urines
δ44/42Ca ICP Ca Lyon (‰)
δ44/42Ca SRM915a (‰)
2.00
1.00
0.00
−1.00
−2.00
Blood (sow)
Bone (sow)
Bone (juvenile)
Colostrum
Milk
Umbilical blood
Urine

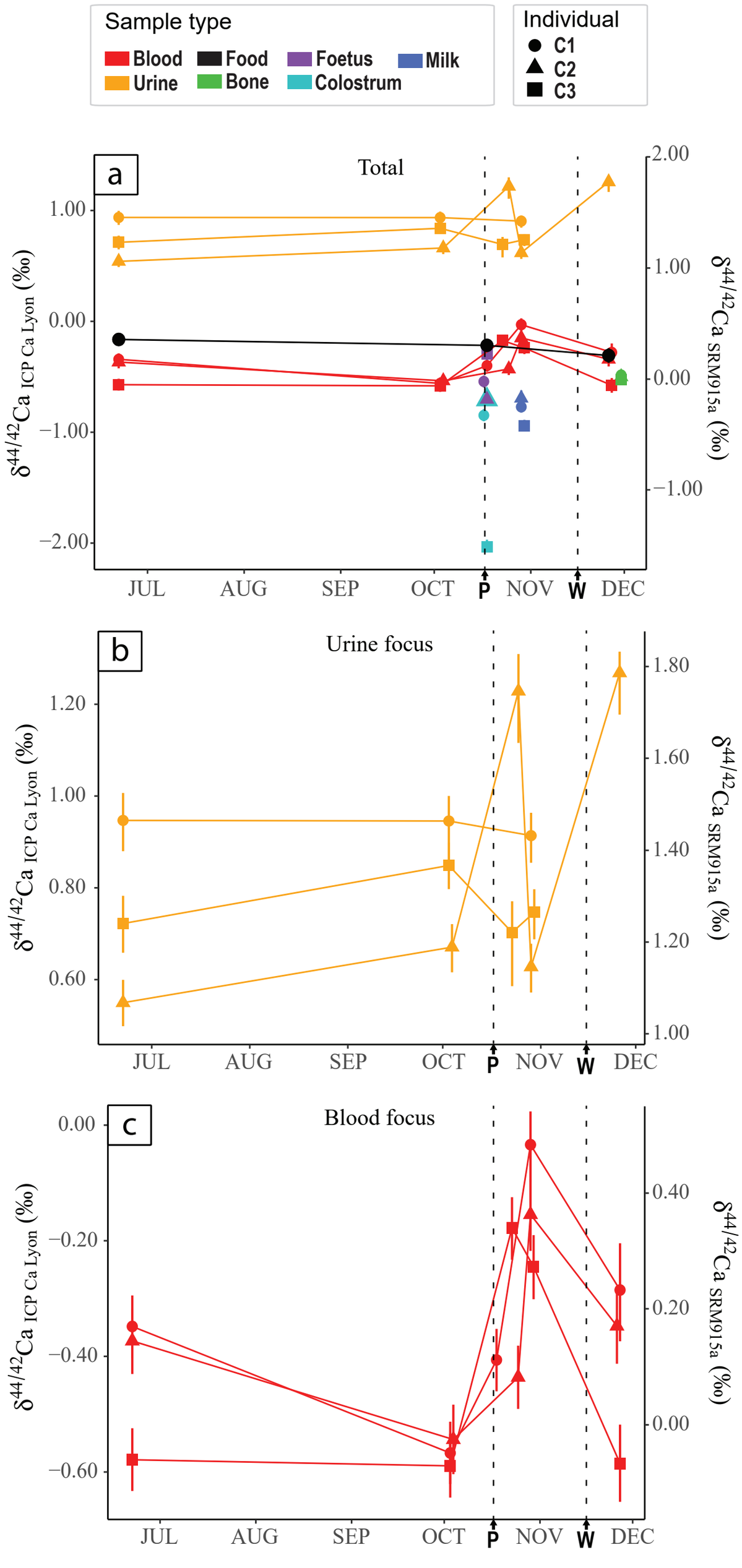
Sample type
Blood
Food
Foetus
Milk
Urine
Bone
Colostrum
Individual
C1
C2
C3
a
Total
b
Urine focus
c
Blood focus
δ44/42Ca ICP Ca Lyon (‰)
δ44/42Ca SRM915a (‰)
JUL
AUG
SEP
OCT
P
NOV
W
DEC

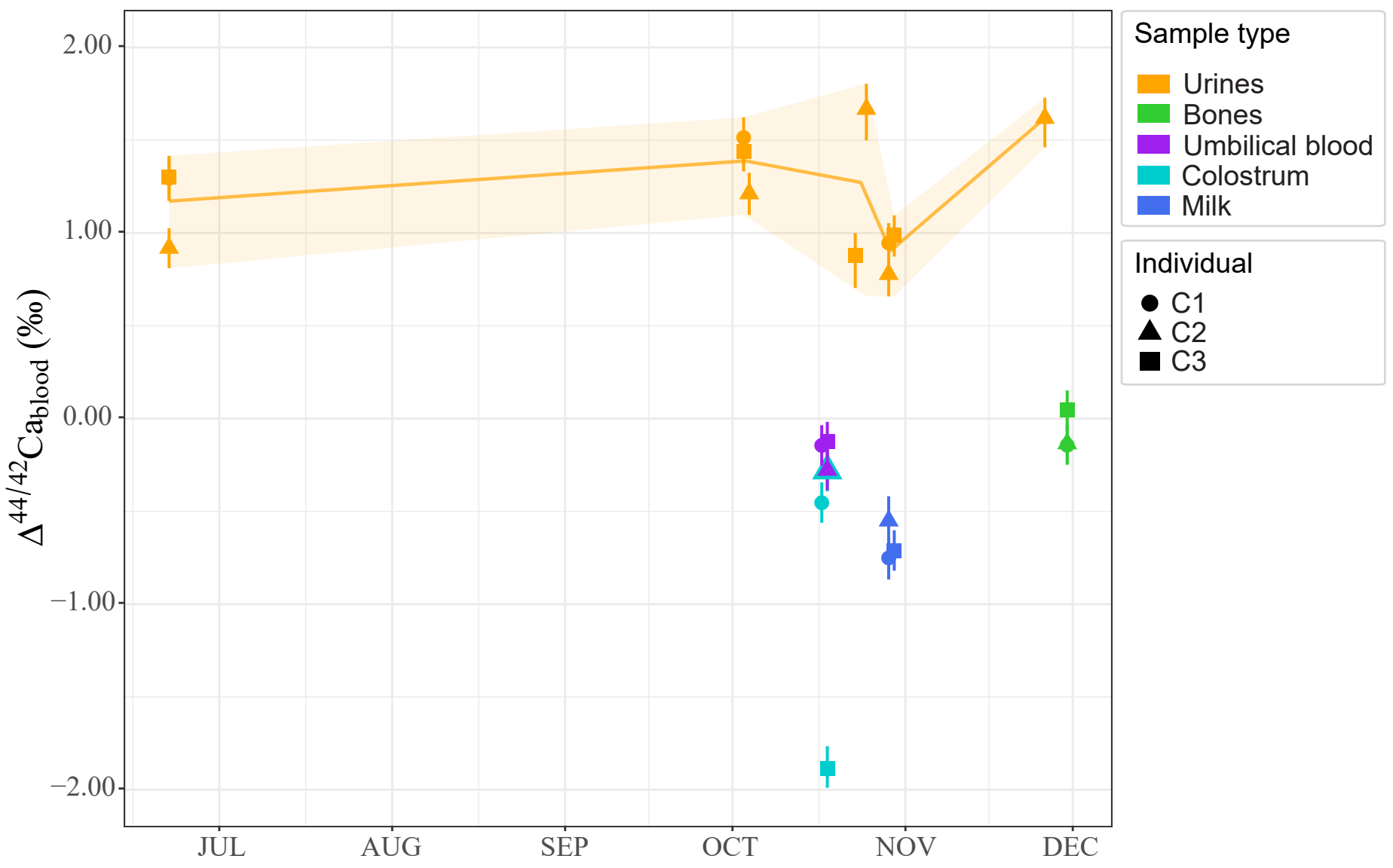
2.00
1.00
0.00
−1.00
−2.00
$\Delta^{44/42}Ca_{blood}$ (‰)
JUL
AUG
SEP
OCT
NOV
DEC
Sample type
Urines
Bones
Umbilical blood
Colostrum
Milk
Individual
C1
C2
C3

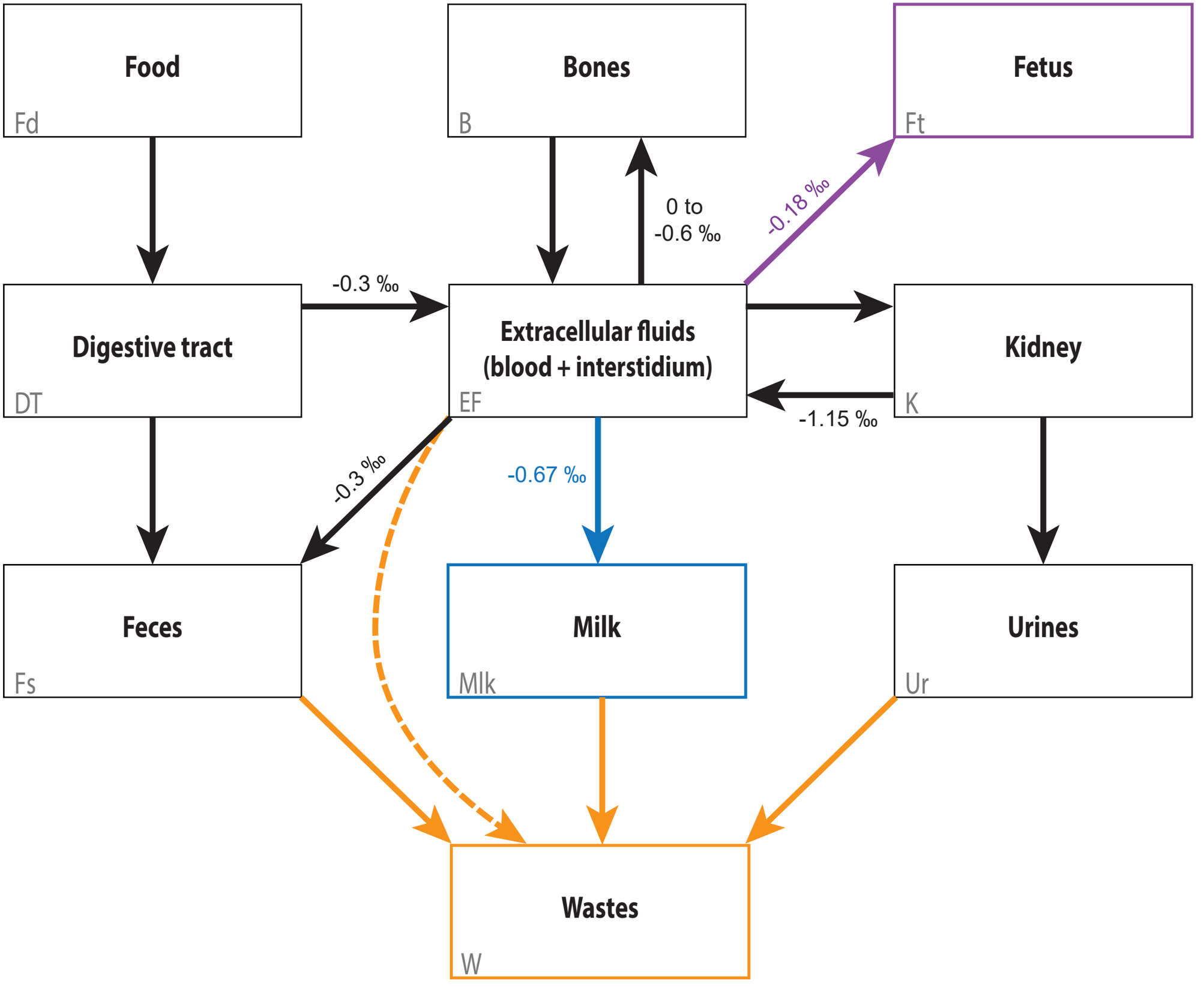
Food
Fd
Bones
B
Fetus
Ft
0 to
-0.6 ‰
-0.18 ‰
-0.3 ‰
Digestive tract
DT
Extracellular fluids
(blood + interstidium)
EF
Kidney
K
-1.15 ‰
-0.3 ‰
-0.67 ‰
Feces
Fs
Milk
Mlk
Urines
Ur
Wastes
W

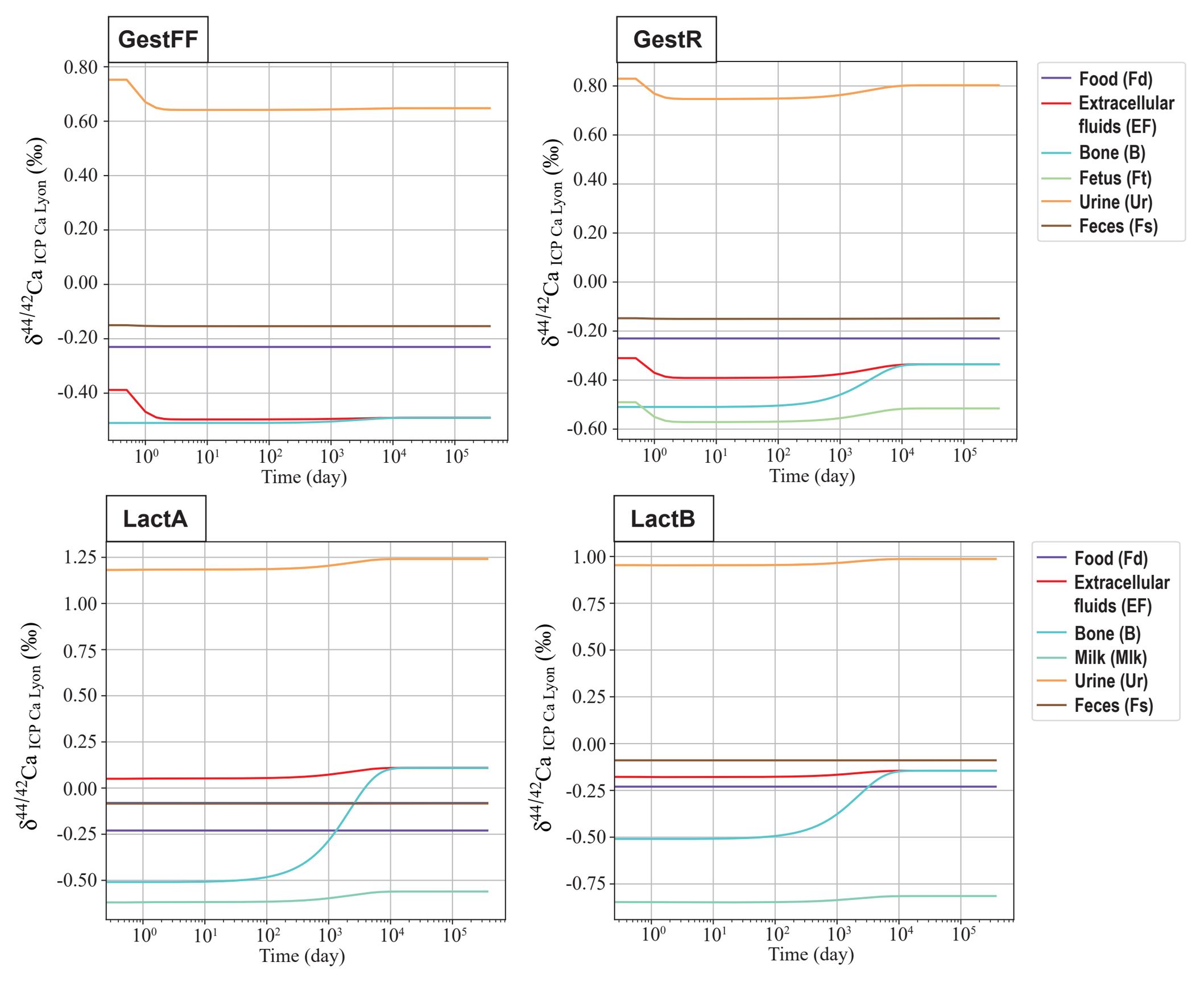
GestFF
GestR
LactA
LactB
$\delta^{44/42}$Ca ICP Ca Lyon (‰)
Time (day)
Food (Fd)
Extracellular fluids (EF)
Bone (B)
Fetus (Ft)
Milk (Mlk)
Urine (Ur)
Feces (Fs)

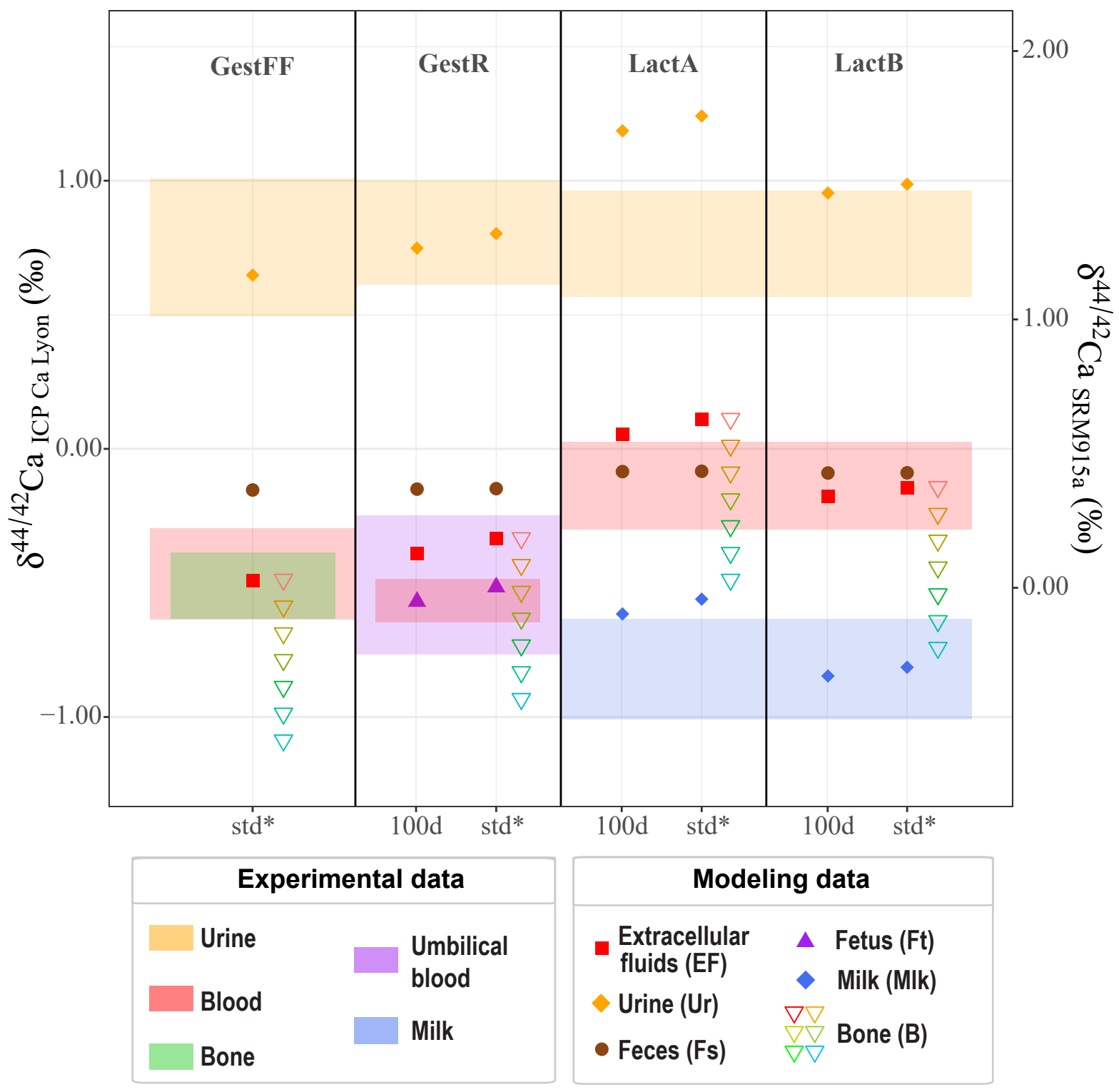
GestFF
GestR
LactA
LactB
1.00
0.00
−1.00
2.00
1.00
0.00
δ44/42Ca ICP Ca Lyon (‰)
δ44/42Ca SRM915a (‰)
std*
100d
std*
100d
std*
100d
std*
Experimental data
Urine
Blood
Bone
Umbilical blood
Milk
Modeling data
Extracellular fluids (EF)
Urine (Ur)
Feces (Fs)
Fetus (Ft)
Milk (Mlk)
Bone (B)

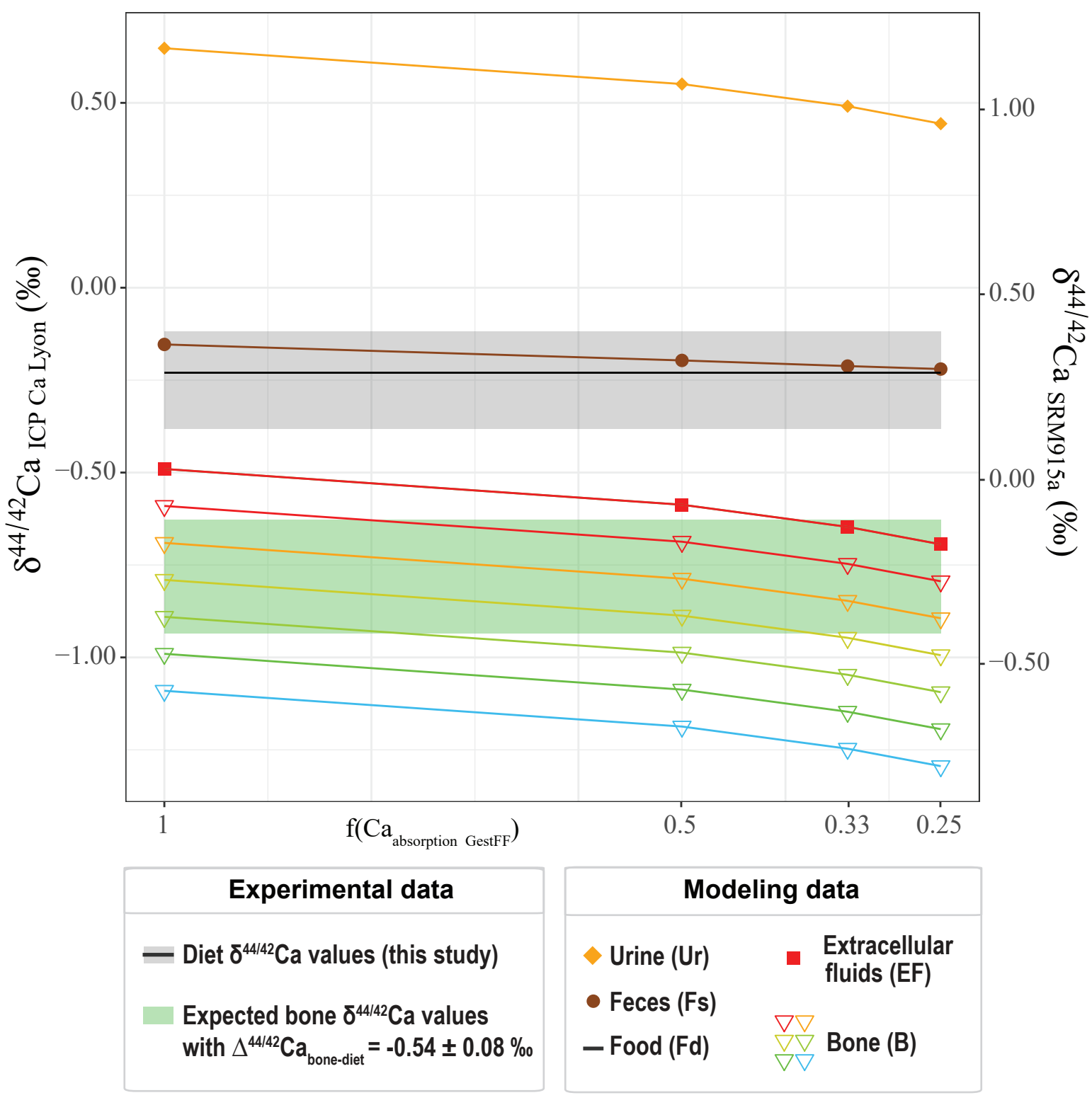
0.50
0.00
−0.50
−1.00
1.00
0.50
0.00
−0.50
δ44/42Ca ICP Ca Lyon (‰)
δ44/42Ca SRM915a (‰)
1
0.5
0.33
0.25
f(Caabsorption GestFF)
Experimental data
Diet δ44/42Ca values (this study)
Expected bone δ44/42Ca values with Δ44/42Cabone-diet = -0.54 ± 0.08 ‰
Modeling data
Urine (Ur)
Feces (Fs)
Food (Fd)
Extracellular fluids (EF)
Bone (B)